PROPERTIES RESEARCH LABORATORY

(2)

PRL 152

SPECTRAL AND TOTAL EMISSIVITY AND REFLECTIVITY AT HIGH TEMPERATURES

Interim Report
(1 Feb 77 - 31 Jan 78)

April 23, 1978

D.P. DeWitt, T.K. Riddle and R.E. Taylor

School of Mechanical Engineering

Purdue University, West Lafayette, Indiana

AIR FORCE OFFICE OF SCIENTIFIC RESEARCH (AFSC)
NOTICE OF TRANSMITTAL TO DDC
This technical report has been reviewed and is approved for publication IAW AFR 190-12 (7b).
Distribution is unlimited.
A. D. BLOSE
Technical Information Officer

PRL 152

Spectral and Total Emissivity and Reflectivity at High Temperatures

Annual Report to

Air Force Office of Scientific Research

Contract 77-3280 New

1 February 1977 - 31 January 1978

by

D. P. DeWitt, T. K. Riddle, and R. E. Taylor

April 1978

ABSTRACT

The status of the high temperature emissometer at the Properties Research Laboratory is described in detail. The emissometer is an extension of the multiproperty apparatus which is a powerful and unique tool for simultaneously measuring ten thermophysical properties on the same sample of an electrically-conducting solid and of studying its behavior under various environmental conditions. The apparatus features rapid time-to-temperature and data acquisition under minicomputer control yielding state-of-the-art accuracy.

Performance evaluation tests of the emissometer are presented. These tests deal with veiling glare, blackbody cavity quality, and temperature distribution in the heating tube and sample. In addition spectral emissivity measurements to at least 10 μm have been made on tantalum (reference material), SiC, Si_3N_4, graphite and carbon-carbon composites from 1500 to 2400 K or their respective degradation temperatures. The new data on the ceramics provides some understanding on their high temperature behavior including the effect of fabrication process and impurities.

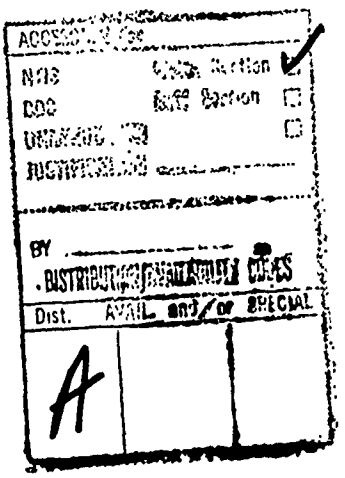

Table of Contents

List of Figures

Figure Page

List of Tables

Annual Report

SPECTRAL AND TOTAL EMISSIVITY AND REFLECTIVITY AT HIGH TEMPERATURES

INTRODUCTION

The goal of this research program is to expand the capabilities of the Multiproperty Apparatus to include measurement of the thermal radiative or optical properties. The Multiproperty Apparatus represents a unique approach for simultaneously obtaining several transport properties. The utilization of the minicomputer to collect observations, control apparatus parameters, and calculate experimental results has been innovative. The method has become widely recognized as the most reliable method for detailed studies at high temperatures.

The thrust of the program for the past two years was the development and evaluation of the "integral blackbody" method for obtaining normal spectral emissivity on electric conductors and on nonmetallic materials. During the first year attention was focused on the method to study metallic systems.

When the sample is an electrical conductor and can be direct electrically heated, the method is readily implemented. In this instance, it is straightforward to assess the systematic errors associated with the quality of the blackbody cavity, temperature gradients in the vicinity of the sample-target areas, and radiometric parameter measurements. The basic features of this method are not new since this approach has been used by

other investigators. However, we have improved the method in two significant ways. First, we are able to simultaneously measure the normal spectral emissivity and other non-radiometric properties such as the hemispherical total emissivity and electrical resistivity. One of the advantages of this feature is the opportunity to characterize the sample surface by measurement of other transport properties. Second, the functions of the minicomputer provide both flexibility in the experimental procedure and improvement in precision over previous investigators.

During the second year of the research program, the subject of this annual report, attention was given to developing a method for measurement of non-metallic materials.

In our method, the sample, in short-cylindrical form, is mounted within a heating tube whose functions are to create an isothermal zone around the sample and to serve as a blackbody cavity. The systematic errors due to temperature gradients in the tube and near the surface (target area) of the sample have been carefully evaluated. This new method has three important features which make it an improvement over other methods which have been previously described in the literature. First, the sample is small and in a form convenient for fabrication; this is especially attractive since new, nonmetallic materials are difficult and expensive to fabricate. Second, the measurement procedure including heat-up time can be accomplished in a short time; this is important in order to reduce effects of the environment on the sample. Third, the heating tube-sample interaction influences are minimized by avoiding solid contact; that is, the sample is thermally coupled by radiation exchange with the heating tube. While some interaction is likely, this can be determined by monitoring electrical resistivity changes of the heating tube in the

vicinity of the sample.

The capability to measure the normal spectral emissivity of non-conductors represents a major contribution to high temperature technology. The existing data in the literature is sparse and poorly characterized (Ref. 1 and 2). For certain classes of materials useful in high-energy, laser-related applications there is insufficient data to even understand temperature effects above normal ambient. Most of the materials are alloys or mixtures and it is expected that higher temperatures (and temperature cycling), environmental conditions (air vs vacuum), and fabrication methods will have an appreciable, if not dominating, effect on the thermal radiative properties. Without the benefit of some careful experimental results on well-characterized materials we are unable to predict such material behavior. As will be seen from the accomplishments of our research to-date, we have the tools to generate high-quality data and new information is being generated which can provide some basis for predictive schemes.

The report is organized to provide a summary of the total program and the measurement capability that exists today. The objectives for the second year are outlined and briefly discussed. A description of the emissometer is concisely presented so that details of the measurement method, hardware and associated minicomputer data acquisition/control system can be appreciated.

In the section entitled "Emissometer Performance Evaluation", we have summarized the activities which relate in some manner to evaluation of the method. This includes the veiling glare effect (scatter) and blackbody quality. Special attention was given to developing a heat transfer model which would permit assessing errors with non-conducting samples due to temperature gradients around the target opening in the heating tube.

The spectral emissivity of tantalum (2-11 μm, 1900K), when compared to existing literature data, serves as means to assess satisfactory performance for metallic samples. Using a new trivalent (Hg-Cd-Te) metal radiation detector, much improved signal-to-noise and longer wavelength operation have been achieved in the past year.

To demonstrate very high temperature performance of the emissometer, a graphite composite sample of proprietary composition (U.S. Naval Surface Weapons Center) was tested. The material failed at 2000K, far short of the 2800K expectation. However, the experience did reveal the need to improve radiation shielding and modify sample configuration in order to achieve very high temperatures without further upgrading of the Multi-property Apparatus.

The primary accomplishment of this year's program is the spectral emissivity data on a collection of commercially available new ceramics, silicon carbide (SiC) and silicon nitride (Si_3N_4). It is shown that the method of fabrication and impurities have a large effect on the radiative properties. This remarkable data set will aid considerably in understanding the basic behavior of materials at high temperatures.

OBJECTIVES OF THE RESEARCH

The second year of the research program was a continuation of our initial activities to develop an emissometer for generating reliable spectral and total emissivity as a function of temperature for selected, well-characterized materials under known environmental conditions. At the outset of the past year, (that is, in our proposal) we identified four objectives as discussed below.

The first objective was to complete base line data (ε_λ) measurements on the nonconducting materials SiC, Si_3N_4, BC and BN. Such data would be generated as a function of temperature with emphasis on approaching melting points; the environment will be vacuum conditons as the aim is to obtain reference data. Commercially-supplied samples for silicon carbide and silicon nitride were available for this study which was completed as proposed.

The second objective was to evaluate the influence of the environmental conditions, primarily air and vacuum, on the emissivity of selected materials. The plan was to modify the Apparatus so that measurements could be performed under controlled atmospheres in addition to the usual high vacuum conditions. We would consider the following: (1) determination of the conditions under which the emissivity is stable for normal atmosphere ambient and (2) the effect of temperature cycling on the emissivity under air and vacuum ambient conditions. Because of the extensive efforts required to complete the first objective, we were unable to begin this work.

The third objective was to study material behavior under dynamic conditions in a controlled environment wherein the sample temperature

would be rapidly changed--over 60 to 120 seconds time period-- from room temperature to near the melting point. Spectral emissivity at selected wavelengths would be measured as a function of time/temperature. For the metallic samples the measurement procedures are relatively straightforward; however, for the nonmetallic "sample-in-the-tube" configuration the transient thermal effects could present serious systematic errors which need to be understood. In our judgement, information on material behavior under these conditions is most appropriate to the high energy laser-material interaction phenomena. Short term oxidation effects under rapidly changing temperatures have not been studied and hence there is no background to appreciate whether a rapid oxidation process will have a greater/less effect on the emissivity of a material than would the slow or static oxidation process we customarily study (our second objective above). The results of this study could have a great impact on directing future laser hardening research. Because of limited resources and higher priorities, this objective could not be considered. It is proper at this point to note that both the second and third objectives are very significant problems which can be readily treated by our tools and research team. We now know it is overambitious to get involved with these studies before the need for reliable, reference data for stable environmental conditions is fulfilled.

The fourth objective involves the continual upgrading of the emissometer to provide the highest degree of reliability consistent with the objectives. Here consideration is given to features of the measurement system and method. New hardware such as a lock-in amplifier and radiation detector (Hg-Cd-Te) were brought on line providing improved measurement precision, and extended operating limits (longer wavelengths and lower

temperatures. Analysis of the non-conducting sample temperature distribution was also performed as a means to better assess the accuracy of the method.

DESCRIPTION OF THE EMISSOMETER

The Multiproperty Apparatus

The experimental apparatus is shown schematically in Fig. 1. The apparatus has been described in detail previously [3] and only a brief description will be presented here.

The metallic sample in the form of a thin-walled, conducting tube is supported vertically between two water cooled movable electrodes as shown in Fig. 2. The non-metallic sample, as shown in Fig. 3., is of a short-cylindrical form mounted with a heating tube. The electrode separation distance is adjustable between 0 and 35 cm. To accomodate length changes in the sample due to thermal expansion a strain-relief system is provided with the lower electrode adjustable. The 76 cm diameter bell jar which contains the sample holder is raised and lowered by power-driven hoist. Vacuum in the low 10^{-6} torr range can be achieved in a few minutes and vacuum in the mid 10^{-7} torr range can be attained with longer pump out times. The bell jar rests on a feed-through collar which contains instrumentation leads, electrical connections and water lines. Signals to be measured are patched into a terminal board connected to the minicomputer. Power is supplied to the sample through regulated DC power supplies. A 500 ampere-50 volt supply, transformer, calibrated shunt, reversing sw switches and remote control circuitry, are used for operations where sample temperatures exceed 1800K while three, 100 amp-10 volt Kepco power supplies are used for lower sample temperatures.

The Optical and Detection System

The emissometer optical system shown schematically in Fig. 4 is

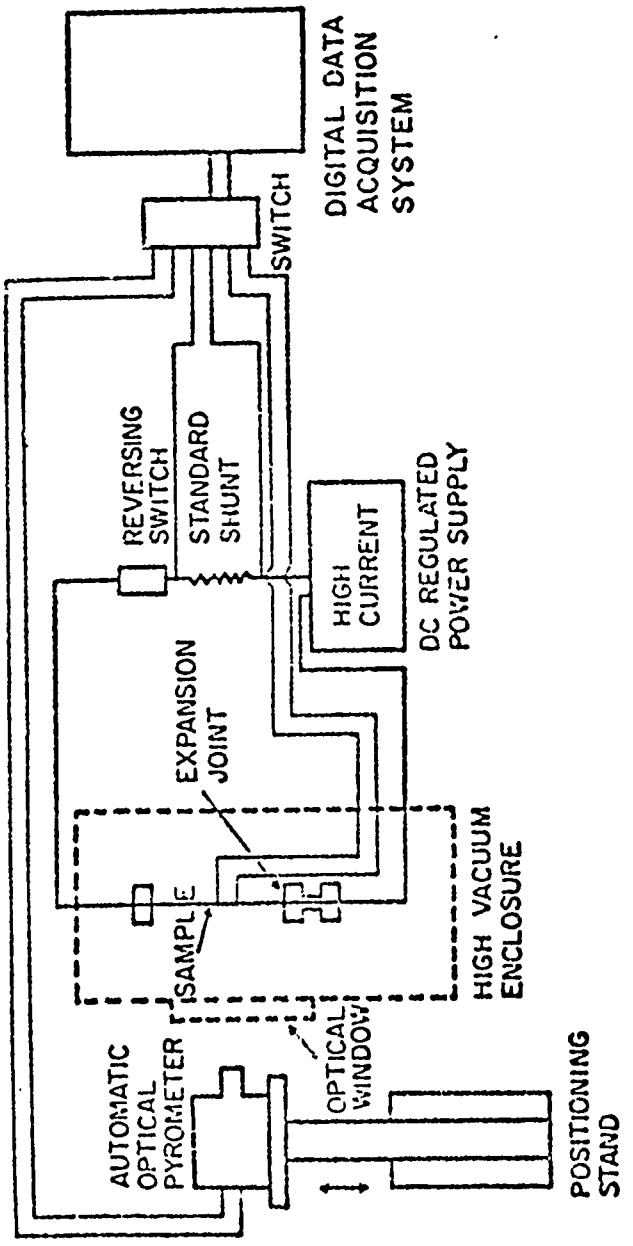

Figure 1. Schematic of the Multiproperty Apparatus

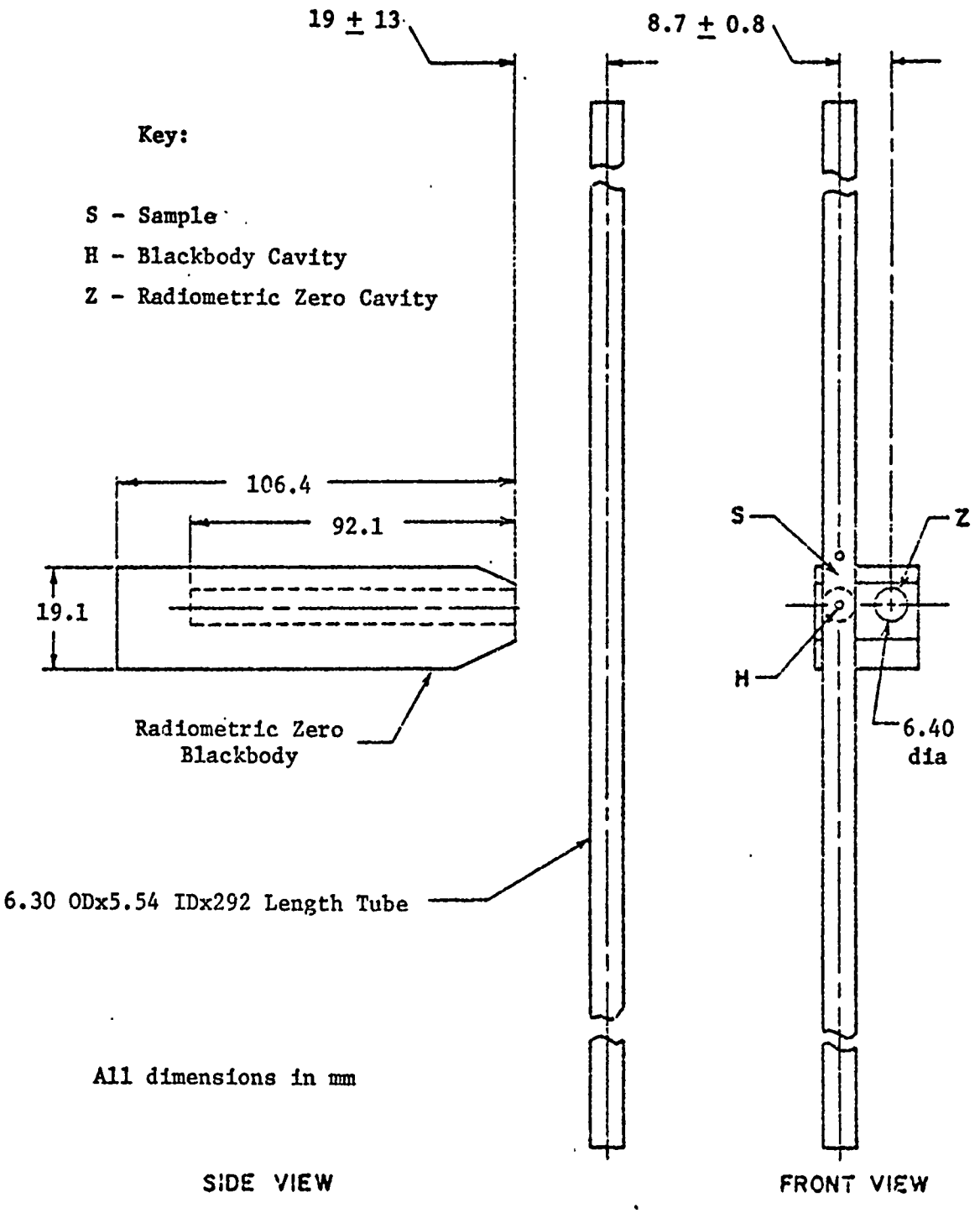

Figure 2. Sample heating tube showing the sample and blackbody cavity target positions within the test section and separate radiometric zero cavity.

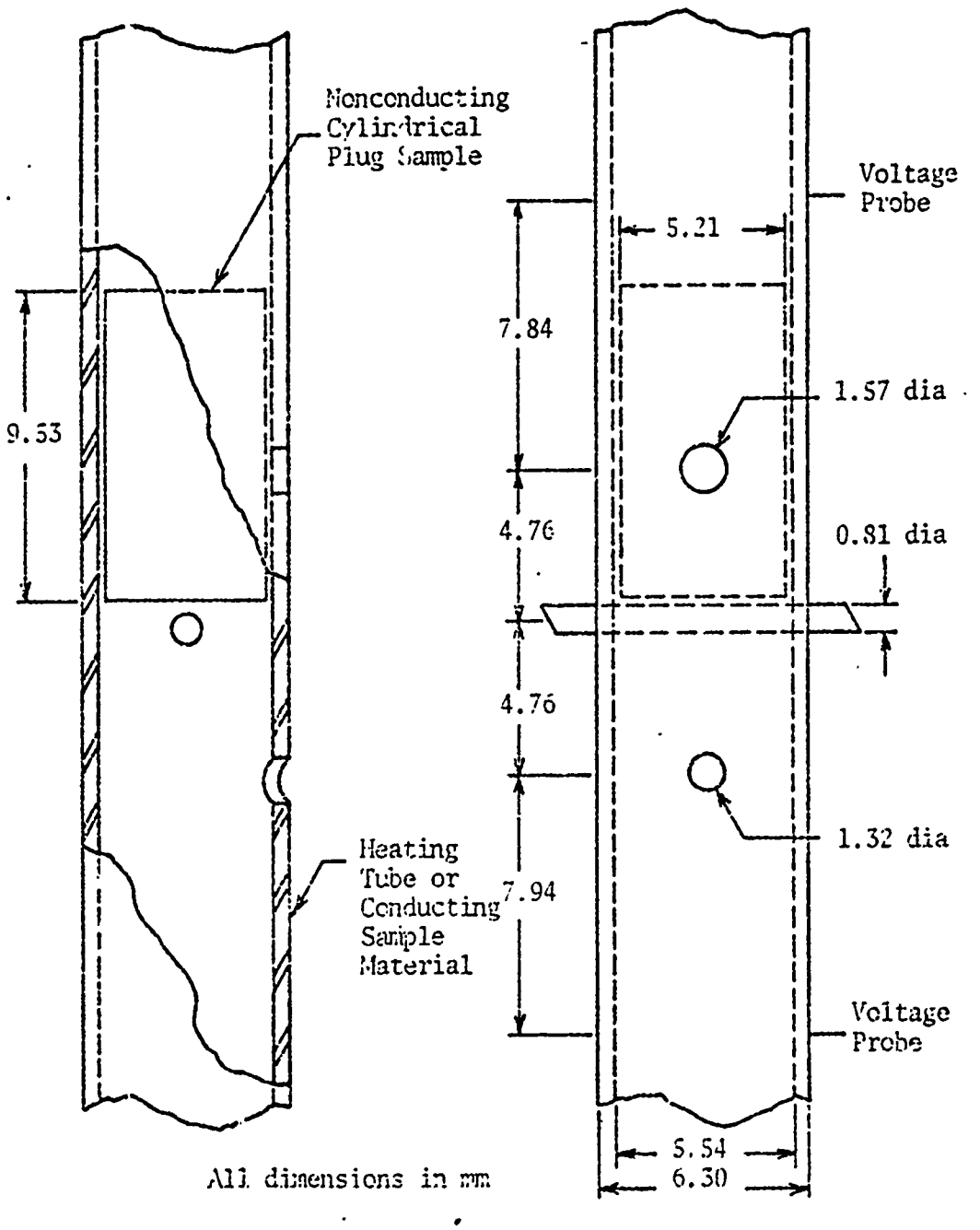

Figure 3. Test section configuration with nonconducting sample (upper cavity) and blackbody cavity.

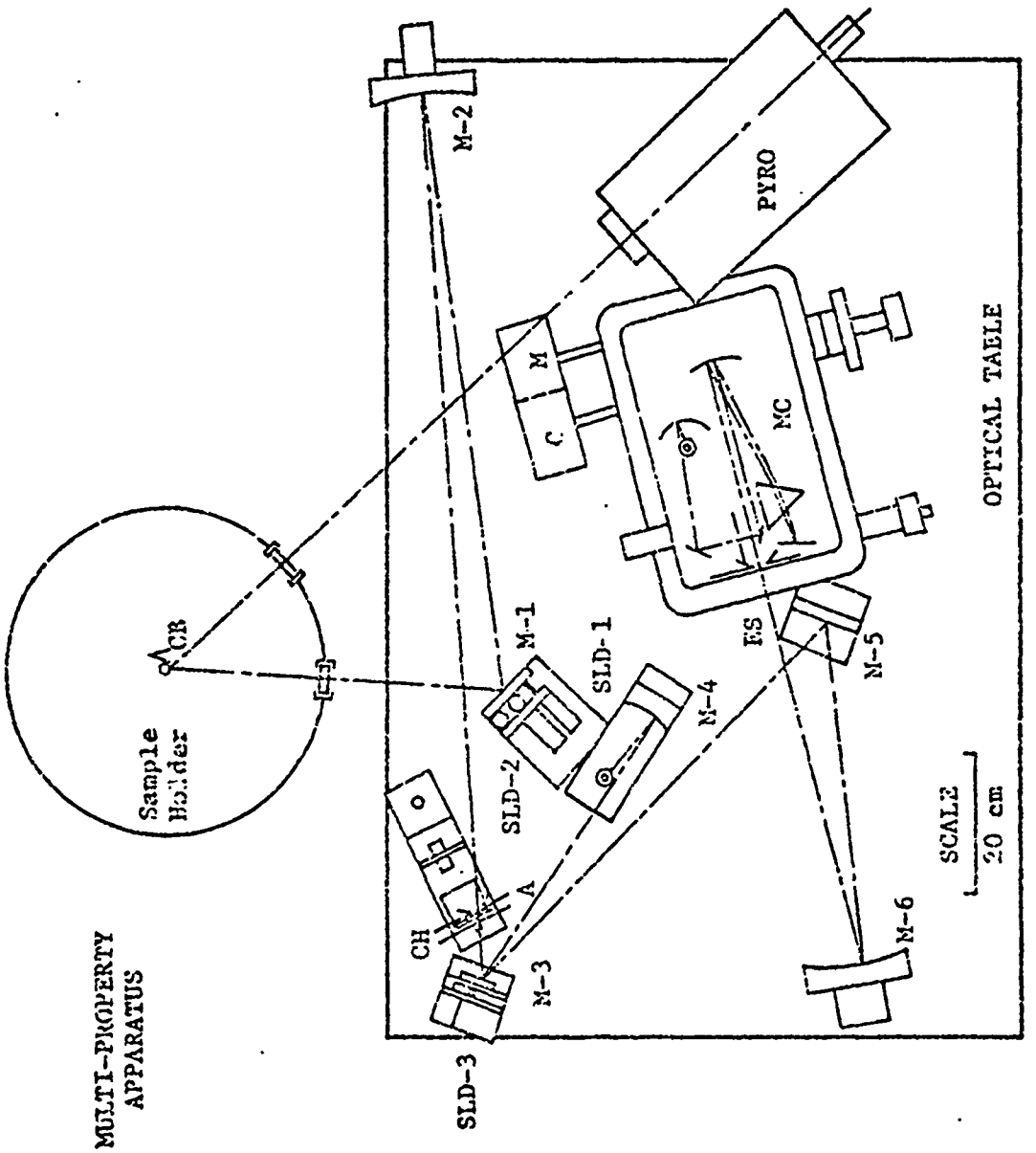

Figure 4. Schematic of the Emissometer illustrating positioning of sample, optical train, and detection system.

mounted on a table located in front of the Multiproperty Apparatus. The position of mirror M1 is set by solenoids prior to the start of the spectral data collection such that signals from the three targets sample surface (S), blackbody cavity (H), and the radiometric zero (Z) - can be measured. During the collection of data the minicomputer controls the solenoids (via programmable switches) such that the three targets are viewed in a time sequence set at the start of the experiment.

The spherical mirror M2 takes the image which is being viewed by M1 (sample surface, blackbody cavity or radiometric zero) and places the image at the aperture (A) plane. A 1000 hz chopper (C) is located just behind the aperture plane.

Mirror M3 can be positioned such that the target image can be placed by the ellipsoid mirror M4 onto a thermocouple detector. In this position the flux reaching the detector is undispersed and the total emissivity can be measured. This feature has not yet been studied. Mirror M3 can also place the target on the plane mirror M5 and then onto the spherical mirror M6. Mirror M6 then places an image of the aperture (A), with a magnification of two, onto the entrance slit of the prism monochrometer, and from here the target image is optically dispersed and focused onto the detector for measurement.

A photograph of the entire optical detection system with the Multiproperty Apparatus in the background is provided in Fig. 5.

The Minicomputer System

The system contains a PDP-8/E minicomputer (central processing unit) with 32,000 words of core connected to an omnibus. Connected to the omnibus through a "data break" is a controller and disk drive for

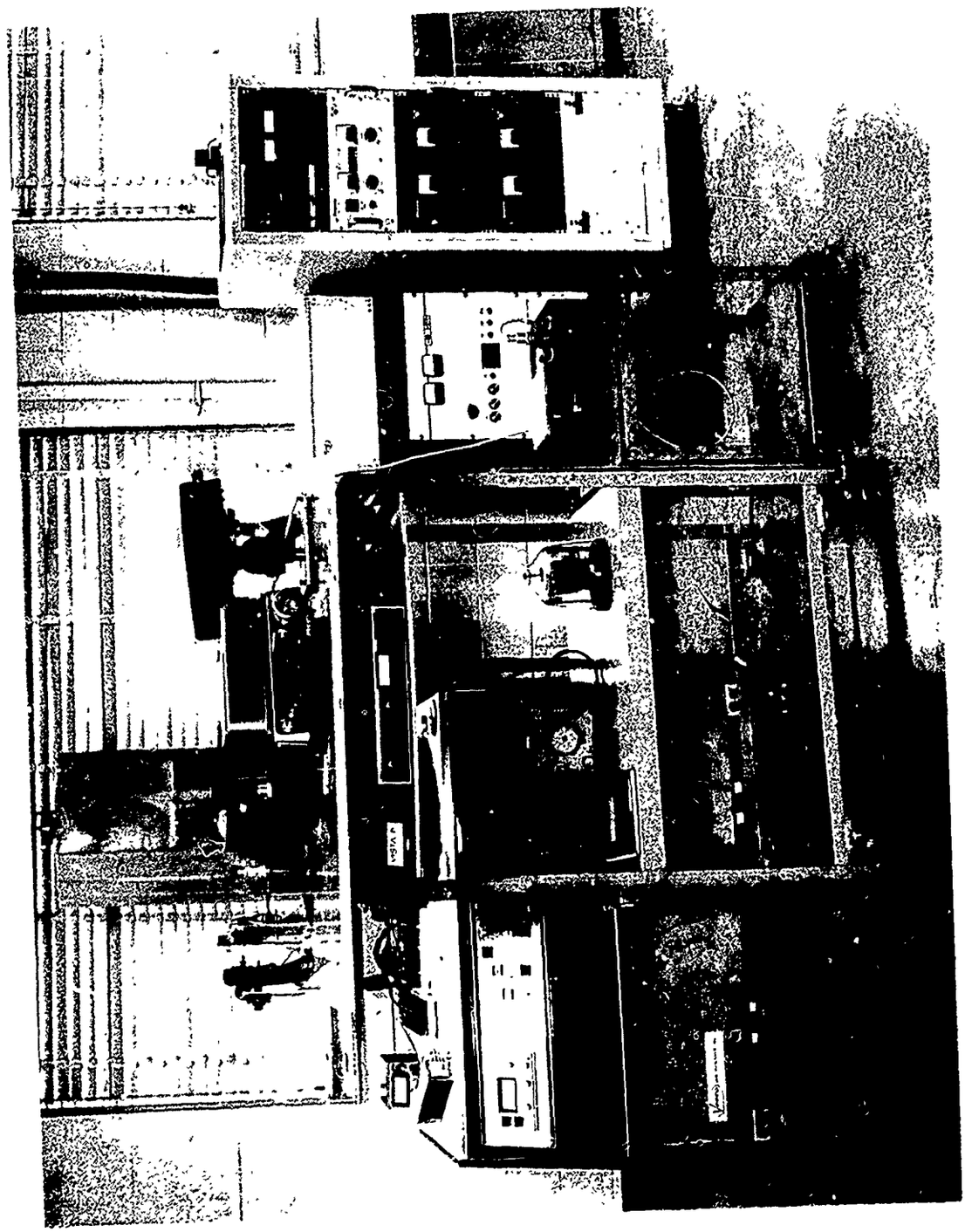

Figure 5. Emissometer showing DC power supplies on the right, Amplifiers in front and the Multi-Property Apparatus in the background.

a disk system which is subdivided into four parts, System (SYS), disk 1, disk 2, and disk 3. The SYS system with $1x10^6$ word capacity and DSK1 with $6x10^5$ word capacity reside on a removable cartridge with a floating head. The other two parts (DSK2 and DSK3 with $1x10^6$ and $6x10^5$ word capacity, respectively) reside on a fixed head cartridge. Information can be swapped readily among the various subdivisions. The capacity of the DDAS is sufficiently large ($3.3x10^6$ words) that programs and experimental data may be stored and used without input-output to any other device such as magnetic tape, punched tape, punched cards, etc., although a high speed paper tape reader/punch and magnetic tape units are included. Other disk cartridges may be readily substituted for the removable cartridge, providing additional storage and back-up capabilities. Instructions and programs may also be entered through the Tektronix Display Terminal (Model 4010-1), which is the master input/output device or through the Decwriter (high-speed teletype) or standard teletype units. The Decwriter is essentially used as a line printer to give printed output. In addition, hard copies of whatever is displayed on the Display Terminal can be made by the Tektronix Hard Copy Unit (Model 4610).

Experimental data are directly entered into the system through an analog-to-digital converter (ADC) or through a VIDAR Model 521-01 integrating digital voltmeter (IDVM). The IDVM is controlled via a master Scanner (Vidar 610) and is equipped for 100 input channels. The Vidar DVM has full scale ranges from 10 MV to 1000 V in steps of 10 and has three integration periods (166.7, 16.7 and 1.67 milliseconds) so chosen as to essentially provide infinite rejection of 60 hz signals. The resolution of the IDVM depends upon the integration period and for the 10 MV full scale range is $\pm$0.1 microvolt for the longest integration

period. Operating in conjunction with the IDVM is a special crystal-controlled timer which accurately records the time the data are taken, without resort to software timing.

In addition; the DDAS is equipped with a real time clock and with programmable switches and digital-to-analog converters (DAC) for controlling experiments.

Details of the measurement procedure and the nature of the software programs have been reported in Reference 4. This will all be omitted for the sake of brevity; however it should be stated that extensive effort was required to develop flexible programs which could be expanded as the emissometer was upgraded.

EMISSOMETER PERFORMANCE EVALUATION

The evaluation of the emissometer has been undertaken in five related studies. In this section, we will briefly present the nature of the various studies and the conclusions reached.

Veiling Glare Study

The veiling glare effect, referred to also as the scattered light effect, is due primarily to dust or other imperfections on optical surfaces such as windows and mirror surfaces. The net effect of veiling glare is to increase the measured radiance value of any target area by the scattering of light, originating from sources external to the target area, into the optical path of the target. From this it should be apparent that the larger the target area is, the smaller the scattered light effect will be, since by increasing the target area, the area external to the target (which is possibly a scattered light source) has been reduced.

The effect of scattered light should be subtracted from the radiance values obtained from the sample surface (S) and the blackbody cavity (H) in the measurement of spectral emissivity. Previous investigators of the integral blackbody method have studied the effects of scattered light and in some cases it was found that substantial errors would result in emissivity values calculated if this effect were neglected. Larrabee, [5,6] for example, concluded that the scattered light correction obtained for his emissometer, lowered spectral emissivity values by 2.5%. However, the diameter of the lateral hole serving as the blackbody was a factor of four smaller than that used in our emissometer. Therefore, in the present study we should expect a smaller, scattered-light correction since our

target size is larger. This comparison is of course assuming that the optical system used by Larrabee is reasonably comparable to that which is used in the present study.

To assess the magnitude of the scattered light effect in the present study, the conducting sample and cold reference blackbody were arranged as shown in Fig. 6. The blackbody cavity (H) shown was formed from a lateral hole placed in the sample surface. In a similar fashion the through hold (TH) was formed by drilling a lateral hole through the front and back surfaces of the tube. The cold reference blackbody (Z) is a water-cooled, graphite block with two cavities each having identical length to diameter ratios. One of the graphite holes is placed directly behind the through hole such that a minimum amount of light will be reflected and scattered into the monochrometer from the region behind the through hole.

The measurement procedure involved the manual positioning of mirror M1 (Fig. 4) to obtain signals from the blackbody cavity (H), the sample surface (S), the through hole (TH) and the radiometric zero (Z). Over fifty signals were averaged at each of the target sights and the standard deviation of each of these averaged values calculated using each of the two equations:

$$\varepsilon_\lambda = \frac{S-Z}{H-Z} \tag{1}$$

$$\varepsilon_\lambda = \frac{S-TH}{H-TH} \tag{2}$$

The (Z) term in calculating spectral emissivity in Eq. (1) is simply to account for amplifier offset. This reading is the averaged amplified detector signal obtained when mirror M1 is positioned to view the cold radiometric zero cavity. The (TH) term in Eq. (2) accounts for both amplifier offset and the effect of scattered light.

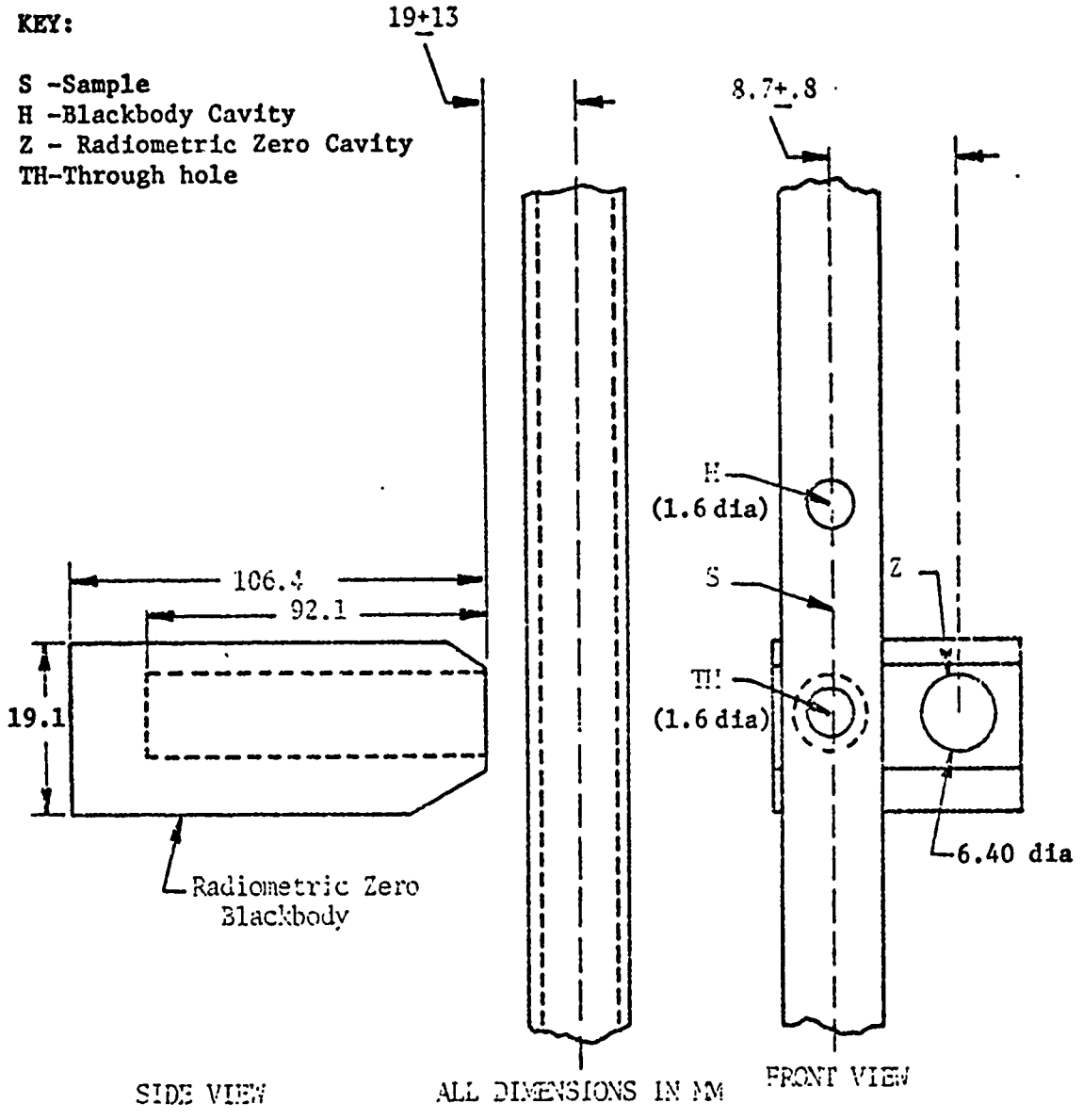

Figure 6. Tantalum tube and cold reference blackbody arrangement used to assess veiling glare effect.

A comparison of the spectral emissivity values calculated using Eqs. (1) and (2) over the spectral range from 2 to 13 μm is presented in Table 1. As can be seen, the spectral emissivity values calculated at each wavelength agree to within the uncertainty of the presented values. Based on these tests, it appears that the measured spectral emissivity value will suffer little or no error if the effects of scattered light are neglected.

Cavity Quality as a Function of Tube Lateral Hole Diameter

The purpose of this study was to determine the dependence of the cavity quality on the diameter of the lateral hole which served as a viewing port for the cavity. Any decrease in the blackbody quality produced by increasing the size of the viewing port would result in an equivalent decrease in the measured blackbody radiance, which would in turn produce an equal increase (error) in the calculated spectral emissivity obtained using Eq. (1). It therefore needed to be demonstrated that the blackbody quality was a weak function of the viewing port diameter through which the cavity was viewed.

Without a nonconducting sample in the heating tube, see Fig. 3, the lower cavity or lateral hole (1.32 mm) acts like a blackbody with a quality estimated to be 0.993. This estimate is arrived at using the DeVos relation [7] assuming that the cavity walls are of uniform temperature over the length of the sample. The effects of interreflections are also neglected in order to simplify the analysis.

The upper cavity shown in Fig. 3 is 20% larger in diameter or 44% larger in area than the lower cavity. Without the sample in position, the DeVos relation estimates the quality of this cavity would be only 0.003 emittance units less than the quality of the lower cavity. This decrease

Table 1

Veiling Glare Study - A Comparison of Emissivity

λ(μm)	Measured spectral emissivity accounting for amplifier offset Eq. (1)	Measured spectral emissivity accounting for scattering and amplifier offset Eq. (2)
2	0.1720 ± .0002	0.1716 ± .0002
3	0.1540 ± .0007	0.1532 ± .0006
4	0.1400 ± .0012	0.1394 ± .0012
5	0.1276 ± .0018	0.1283 ± .0026
6	0.1243 ± .0014	0.1238 ± .0014
7	0.1072 ± .0027	0.1056 ± .0024
9	0.0878 ± .0066	0.0873 ± .0079
11	0.0678 ± .0123	0.0669 ± .0111
13	0.0574 ± .0324	0.0506 ± .0280

in quality can be evaluated experimentally. A tantalum tube was heated to 1800K and radiation thermometer observations were taken of the upper and lower cavities. The lower (smaller) cavity was assumed to have a quality of unity such that the spectral radiance temperature measured for this cavity gave the true temperature of the tantalum tube. The quality of the upper cavity was then determined from the well-known Wien's law expression:

$$\varepsilon_c(\lambda_e) = \exp\left|\frac{C_2}{\lambda_e}\left(\frac{1}{T} - \frac{1}{T_s}\right)\right| \qquad (3)$$

where λ_e is the effective wavelength (0.65 μm), C_2 is the Second Radiation Constant (14388 μm-K), T_s is the spectral radiance temperature of the cavity in question, T is the temperature, and ε_c is the sought-after emissivity at 0.65 μm. From this the quality of the upper cavity was determined to be 0.010 units less than the lower cavity instead of 0.003 units as predicted by DeVos. This difference can be explained by the combined precision of the radiation thermometer and the variation of the observed radiance temperature when sighting into either of the cavities; this amounts to nearly 0.005 units.

This study shows that increasing the hole surface area by 44% decreased the quality by less than 1%. It was therefore concluded that the size of the hole, at least within the diameter range considered here, has very little effect on the quality of the blackbody and therefore very little effect on the measured spectral emissivity.

Cavity Quality with Nonconducting Sample Present

The objective of this study was to determine how the quality of the lower lateral hole in the heating tube (Fig. 3) was effected by the

presence of a nonconducting cylindrical sample. It is possible that the quality of this cavity would be dependent upon the emissivity of the sample since the cavity is bounded at the upper end by the sample. The geometry of this configuration is rather complicated and analytical treatment to predict how the cavity quality is altered by the presence of the sample would be difficult.

An experimental procedure to estimate how the quality of the lower cavity is altered by the sample was developed. This method assumes that the quality of the lower cavity without the sample in position is unity. The experimental approach relies on the use of the tantalum heating tube as a resistance thermometer. The cross-section areas and density of the tantalum tube as shown in Fig. 3 are carefully determined. Voltage probe leads are spot welded to the tantalum tube and the distance between probes accurately determined. In a separate apparatus, the room temperature resistivity is determined for a section other than that between the voltage probes and compared with the resistivity between the probes. Typically, the effect of the four holes (cavities plus pin holes) in the test section is to cause an increase of 1% in the apparent resistivity of the tantalum.

The heating tube, without a sample in position is brought to an operating temperature as determined by sighting with the radiation thermometer, into the lower cavity. The electrical resistivity of the test section was then determined from observations of the voltage drop across the test section and current through the tube. The solid line of Figure 7 represents a least-squares, linear fit to a series of resistivity-temperature measurements taken around 1800K. Reference [8] gives the temperature-resistivity relationship for tantalum as:

$$r_e = (\mu\Omega\text{-cm}) = A+BT+CT^2 \qquad (4)$$

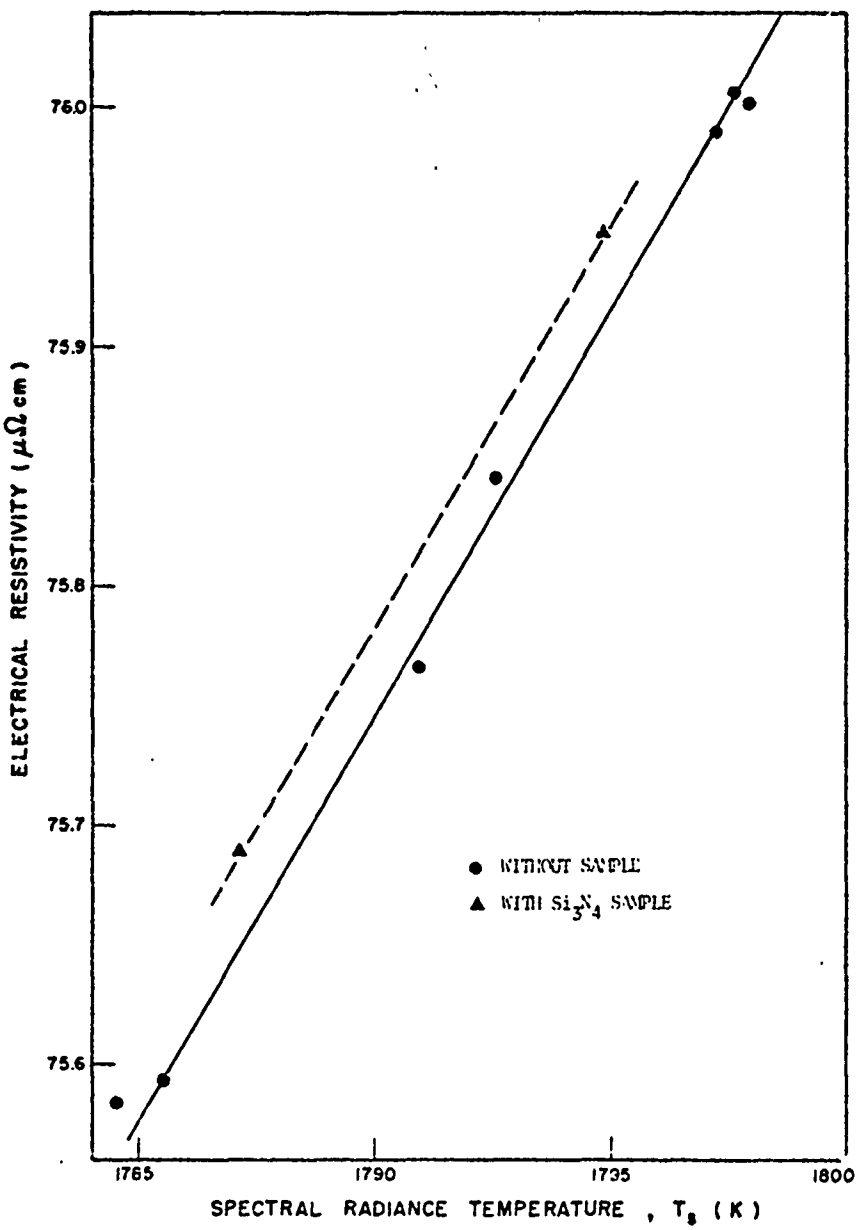

Figure 7. Lower cavity quality determination with silicon nitride sample in position from spectral radiance temperature, T_s (0.65 μm), and electrical resistivity observations.

where T is in kelvins and the values of the coefficients are A=4.43633, B=4.1944 x 10^{-2}, and C=2.3220 x 10^{-6} for the temperature range from 1000 to 2800K. The coefficients for our tantalum tube differ by a few percent from the values of Reference [8] for reasons of higher impurities and some ambiguity in the tube dimensions (cross-sectional area) and effective length between the probes. However, for the limited temperature range and tube configuration, the relationship between the resistivity and temperature has been established; knowing this relationship, the tantalum heater tube can now be used as a resistance thermometer.

A nonconducting cylindrical sample is next inserted into the heating tube and the current carefully adjusted to very closely match the resistivity that was used in the "tube only" test, it is then assumed that the test section is at the temperature determined from the measured resistivity and the resistivity-temperature relationship. The spectral radiance temperature, T_s, of the lower cavity is then measured with the radiation thermometer. For the sample materials used, the observed spectral radiance temperature of the lower cavity as a function of electrical resistivity is represented by the dashed curve, Fig. 7. This curve has the identical slope as the solid curve representing the tantalum heating tube "resistance thermometer" relation. The temperature offset of the two curves can be used to calculate the emissivity of the lower cavity with the silicon nitride in place. For this, Wien's law expression, Eq. (3), is used assuming that the lower cavity has a quality of unity when the sample is not present. The results of these observations and calculations for two nonconducting materials; silicon carbide and silicon nitride, are summarized in Table 2. Also shown in the table are the measured spectral emissivity values for these materials. The conclusions reached from these results are that the

Table 2

Cavity Quality with Nonconducting Sample Present

	Spectral Emissivity (0.65 μm, 1800 K)		
Target Cavity	Without Sample	With Sample	
		SiC	Si_3N_4
Upper	0.990	0.801	0.654
Lower	1.000	0.993	0.994

presence of the sample has little effect on the quality of the lower cavity and that the effect of the sample emissivity on the quality, at least for the emissivity range herein studied, is negligible. It should be noted that the quality is not likely to be a function of wavelength provided spectral emissivity values do not change markedly.

Heating Tube Temperature Distribution with Sample Present

The purpose of this study was to measure the longitudinal temperature distribution of the tube with the sample present, in order to assure that the test section remained isothermal when a sample was placed in the heating tube (Fig. 3). The influence of the sample on the temperature distribution of the tantalum heating tube at 1800K can be seen in Fig. 8. The spectral radiance temperature (0.65 μm) observations were taken under matched electrical resistivity conditions for "without" and "with" sample configurations; that is, the average temperature between the voltage probes is the same for each configuration. The general trend is that the sample has not really altered the temperature distribution. The temperature differences, particularly for the "with sample" case, are most likely due to emissivity variations resulting from grain boundaries and minor imperfections on the tantalum tube surface. This can be fully appreciated when noting that the radiation thermometer target diameter is 0.5 mm dia and that the total temperature range difference between the two configurations can be explained by a $\pm$0.010 emittance unit variation of the tantalum surface. That is, the spectral radiance temperature distribution is more likely explained by variations of emissivity than by a difference in temperature for the two configurations. It is for this very reason that it is necessary to use the present resistance thermometer approach rather than a radiation thermometer observation on the tantalum surface to determine the

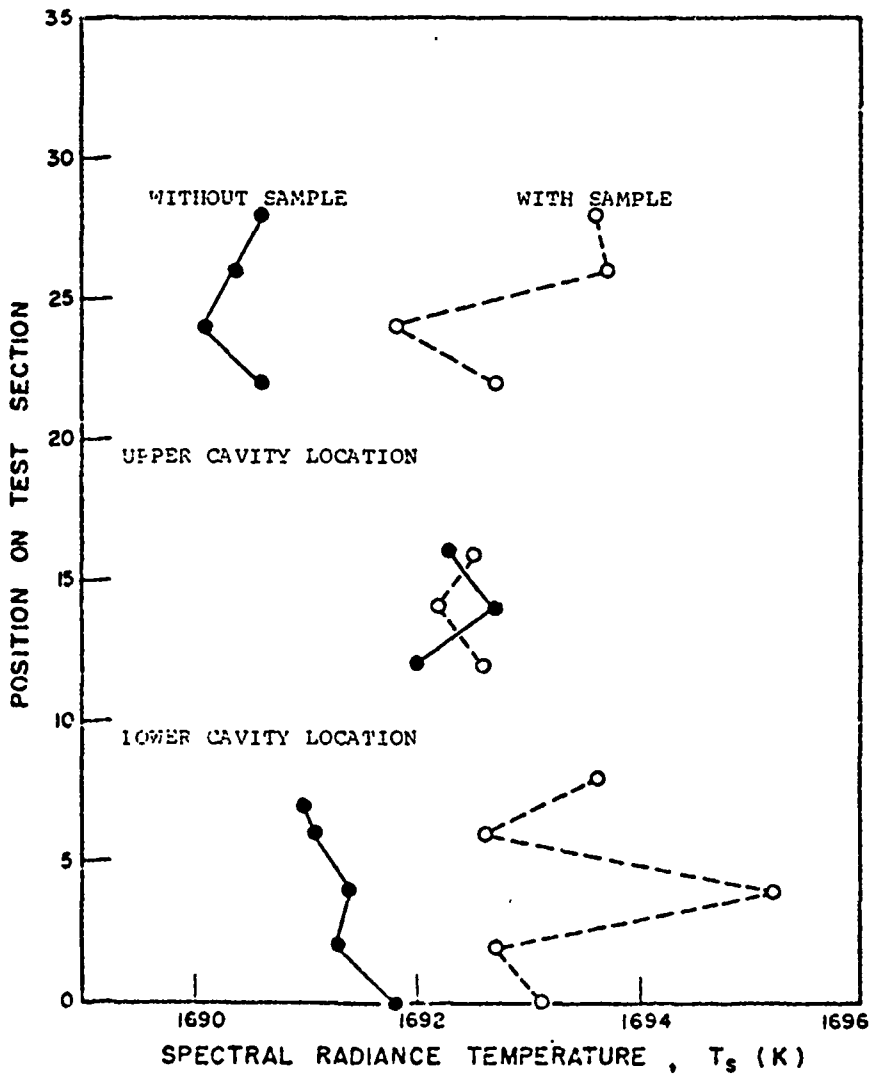

Figure 8. Tantalum heating tube spectral radiance temperature distribution, T_s (0.65 μm), with and without a silicon carbide sample in position.

average temperature of the test section. From this we then conclude that the test section comprised of the sample and the lower cavity blackbody meets the isothermal requirements to determine emissivity without significant error.

Sample Temperature Distribution

It is essential that the surface temperature distribution be nearly uniform for the nonconducting sample inside the heating tube (Fig. 3). A heat transfer model was developed to predict the temperature distribution on the surface of a nonconducting sample mounted with the heating tube assumed to be isothermal in the longitudinal direction. Figure 9 shows important details of the model and an indication of how the numerical solution is treated. The lateral hole opening through which the sample is observed is r_o, the tube temperature is T_o and the sample material properties required are the thermal conductivity, k, and the hemispherical total emissivity, ε.

The spacing between the sample and the tube, h, was found to have very little effect on the sample temperature distribution. This result was very informative since it had earlier been thought that the sample needed to be fitted very closely to the inner diameter of the tube to achieve uniform temperature conditions.

The effect of the tube temperature, T_o, on the nonconducting sample surface temperature distribution is shown in Fig. 10. The ordinate, T_o-T, is an indication of the temperature depression of the nonconducting sample at the center of the lateral hole opening. The valu for k, r_o, and ε are typical of those encountered for materials in our program.

To determine the error produced in measured spectral emissivity values due to the temperature depression of the nonconducting sample, Fig. 11

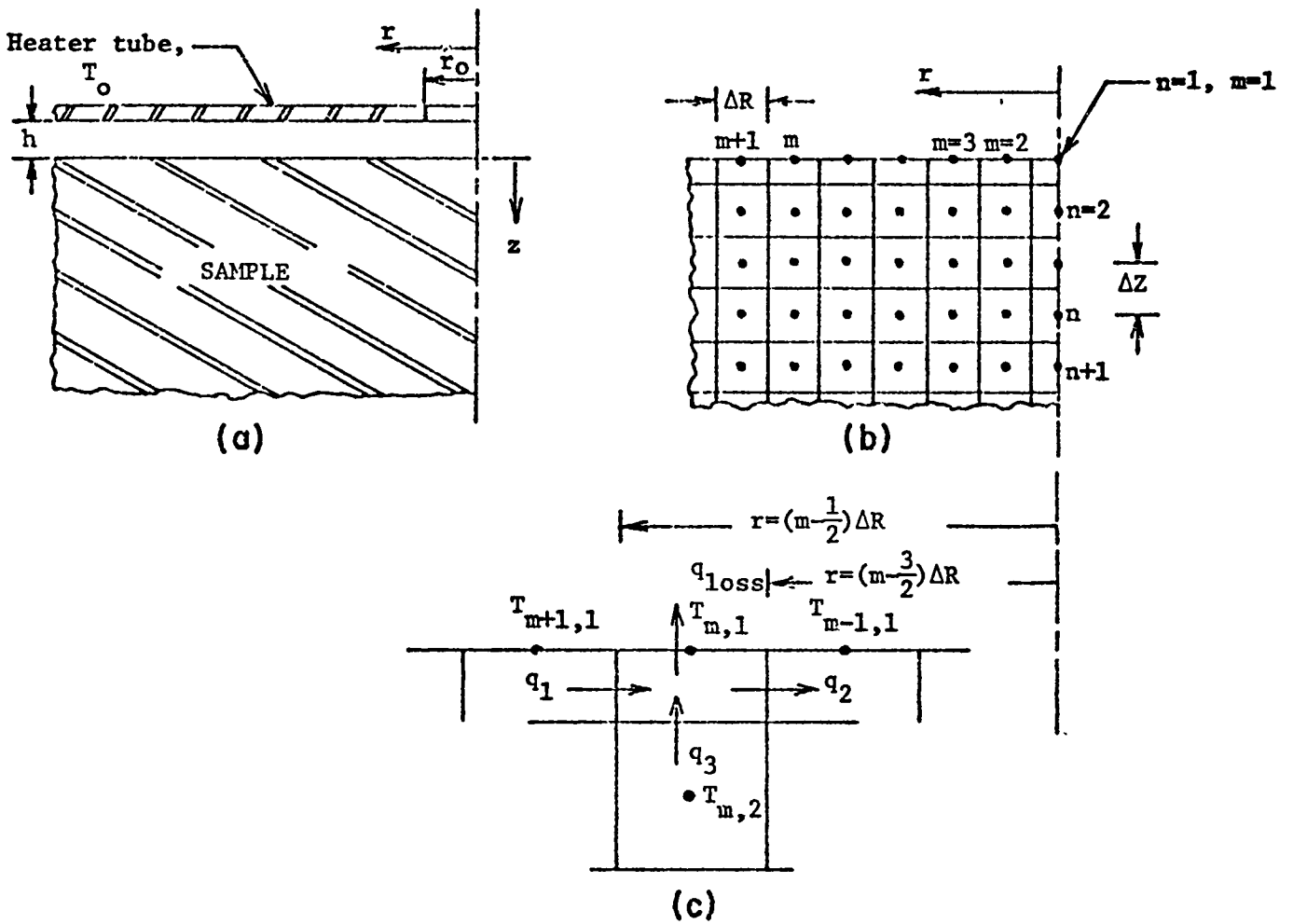

Figure 9. Important variables used in nonconducting sample model:

a) cross-sectional view of sample in heating tube;
b) nonconducting sample nodal arrangement; and,
c) typical surface nodal element

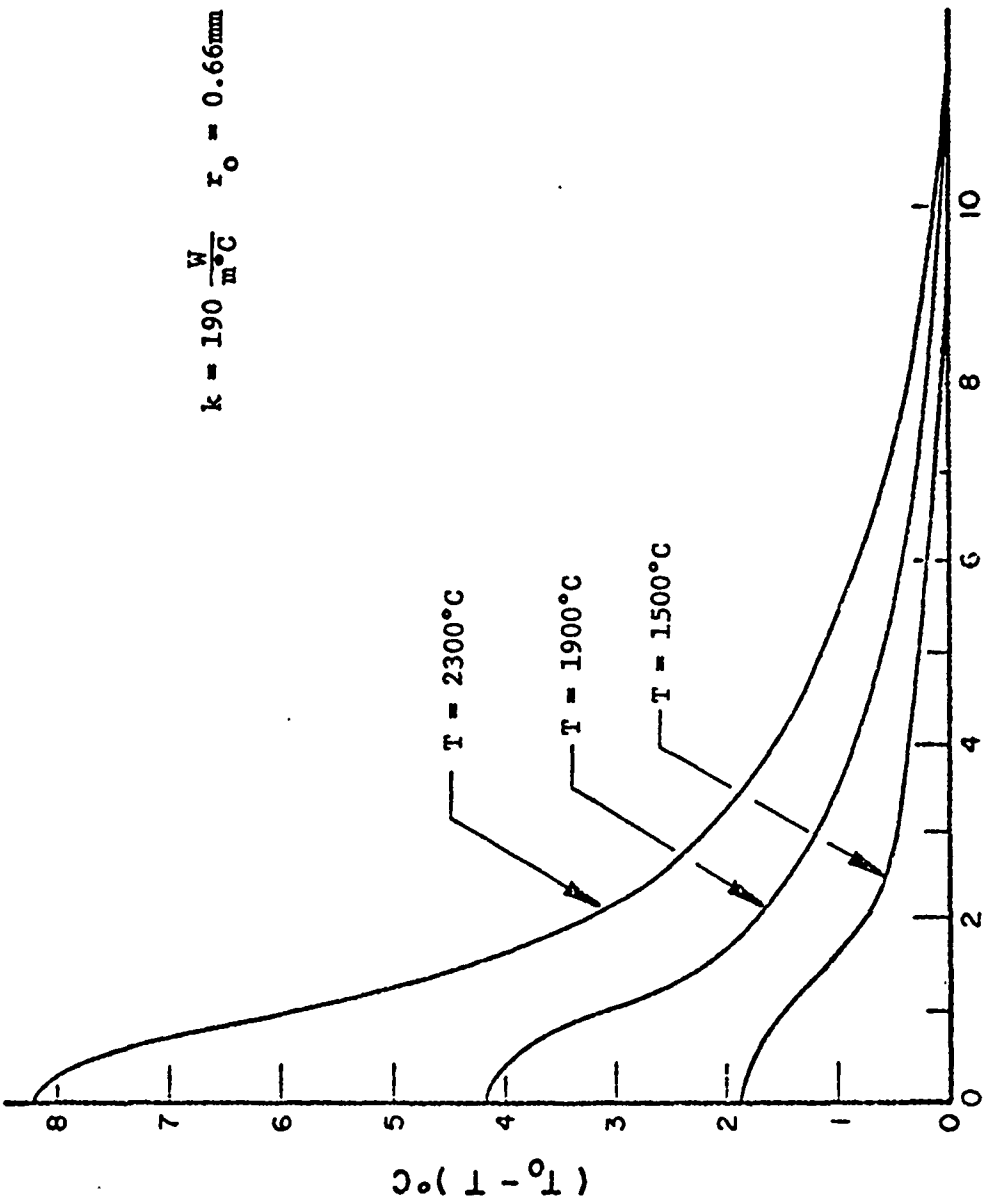

Figure 10. Nonconducting sample surface temperature distribution as a function of heating tube temperature.

can be used. For a specific wavelength λ, (μm), and heating tube temperature T, (kelvins), this figure gives the percentage blackbody spectral radiance error, $\Delta L_{b\lambda}/L_{b\lambda}$ (%) produced by a temperature difference between the sample and the blackbody, ΔT (or $T-T_o$ from Fig. 10). This error in the blackbody spectral radiance value produces an equal error in the calculated spectral emissivity.

To illustrate the use of these figures, consider the T=1500°C curve of Fig. 10. The maximum temperature depression (r=0) is 1.8°C; this corresponds to a $\Delta T/T = 1.8/1500 \approx 0.1\%$. So for the worst spectral case we encounter, λ=2μm; this corresponds to a λT product, 2μm x 1773K = 3546μm-K. From Fig. 11, we see the spectral radiance error is estimated as 0.5%. For a tube temperature at 1900°C this error is 0.8% and at 2300°C, the error is 1.3%. The errors predicted for heating-tube temperatures in the range 1900 to 2300°C presently represent worst-case conditions since the nonconducting sample materials with which we are concerned in this study, namely SiC and Si_3N_4, would not be able to withstand temperatures greatly in excess of 1900°C without failure.

Additional results from the model are shown in Fig. 12, for the influence of the sample material properties (ε,k) and in Fig. 13 for the effect of lateral hole opening r_o. These results are useful for estimating how sample and tube parameters can likely influence the observed spectral emissivity data.

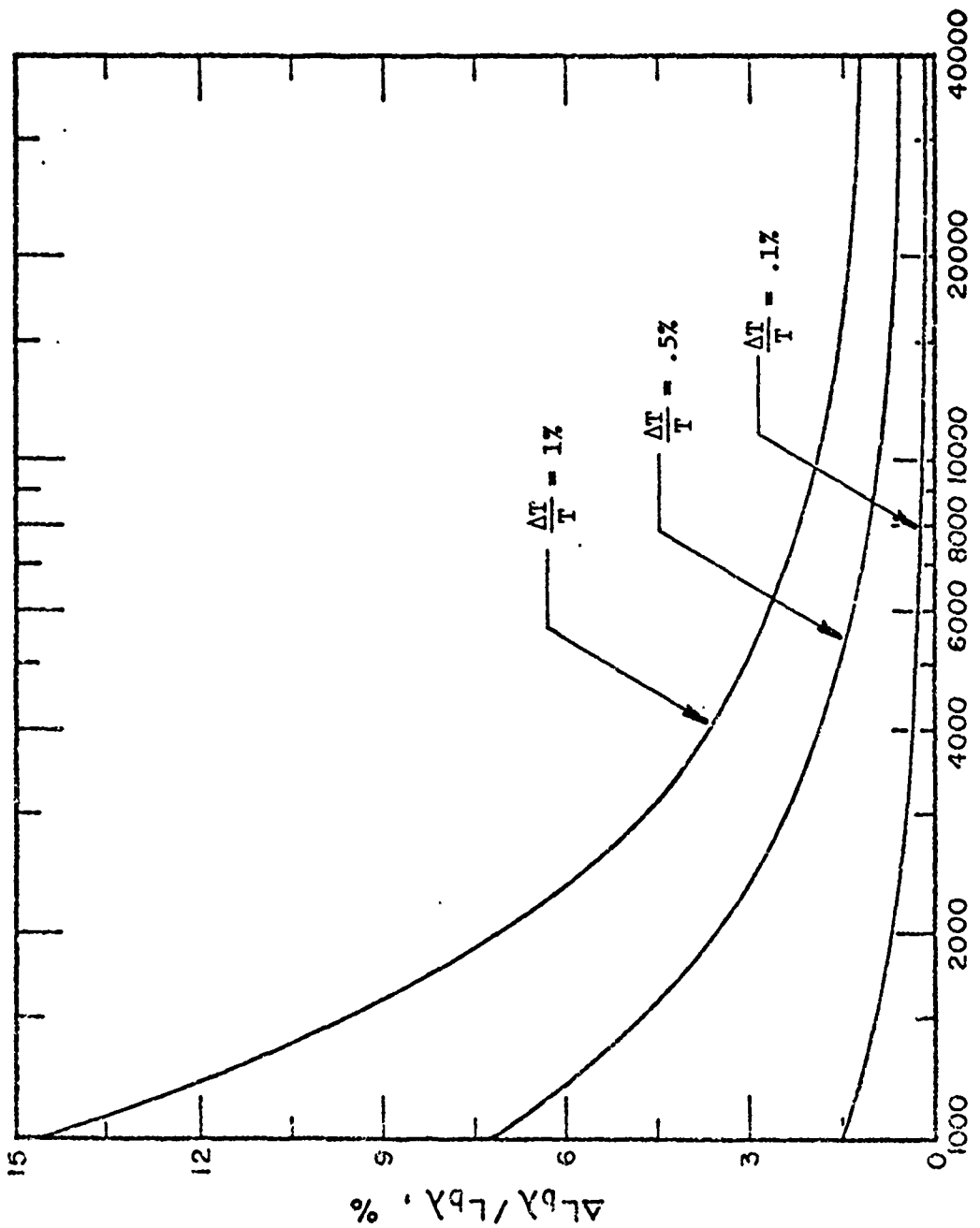

Figure 11. Blackbody spectral radiance error as a function of wavelength (λ), heating tube temperature (T), temperature depression of nonconducting sample at its observation point (ΔT).

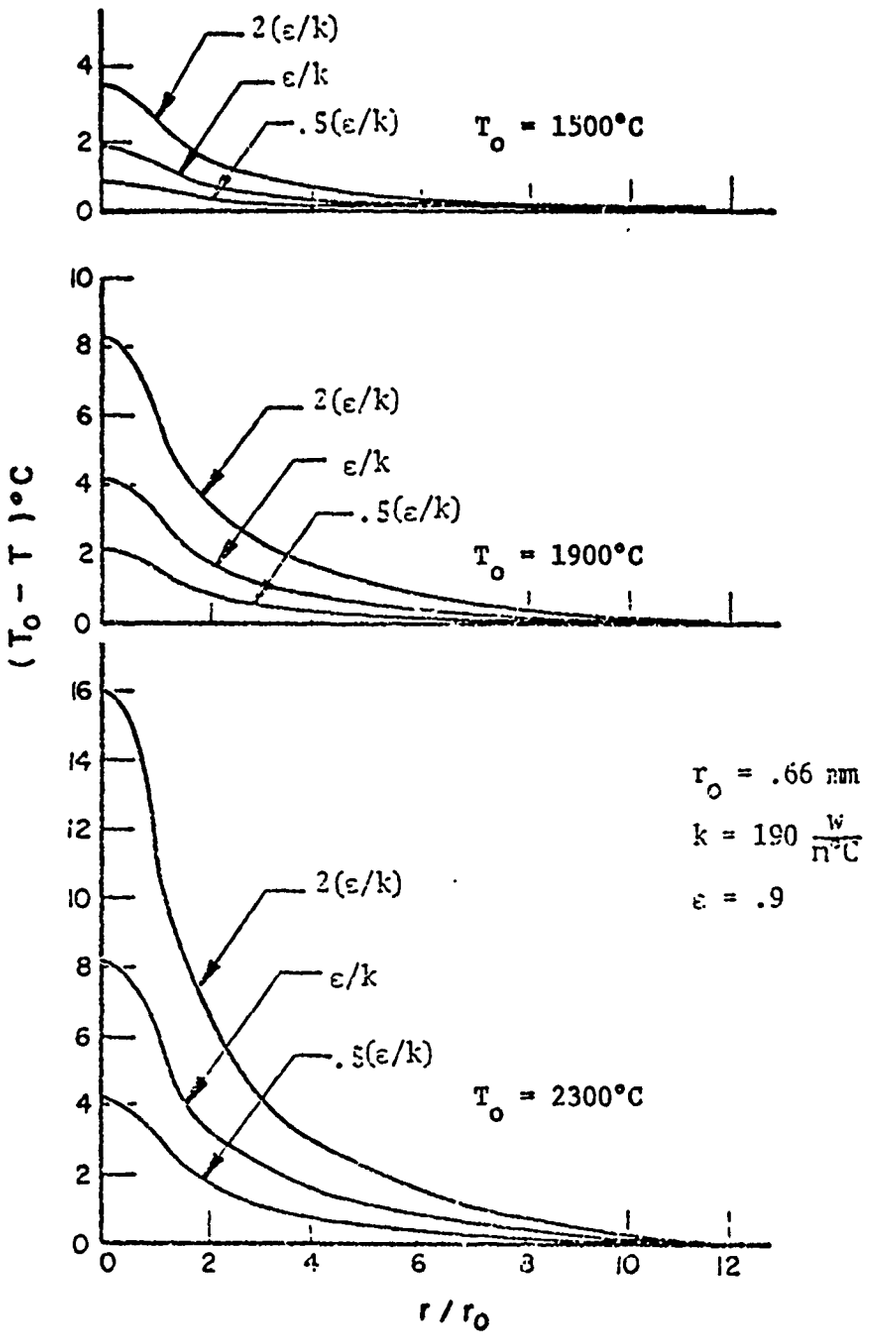

Figure 12. Nonconducting sample surface temperature distribution with the sample emissivity to thermal conductivity ratio as a parameter.

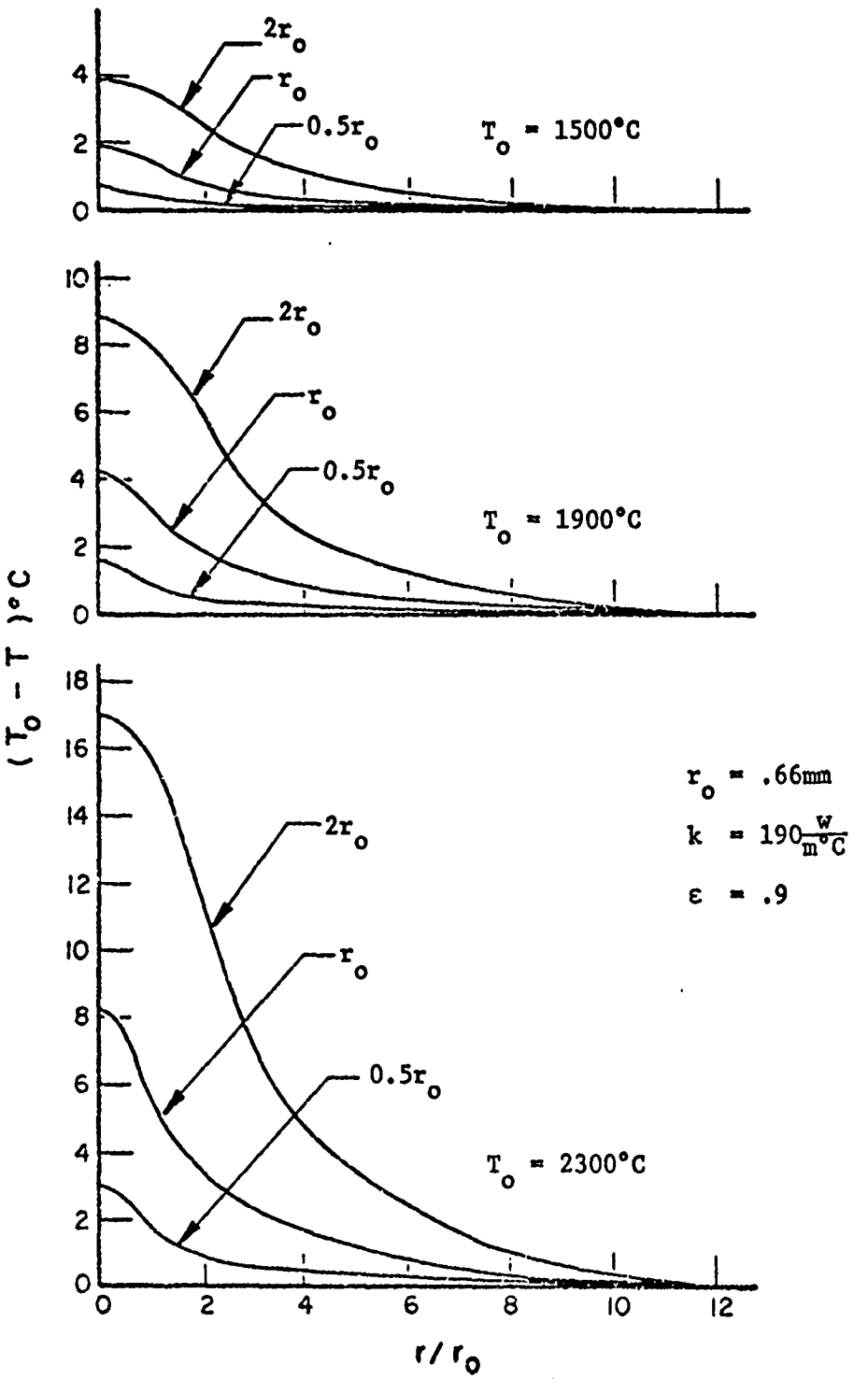

Figure 13. Nonconducting sample surface temperature distribution with lateral hole radius through which nonconducting sample is viewed as a parameter.

SPECTRAL EMISSIVITY OF TANTALUM

To evaluate emissometer performance with electrical conducting samples, measurements were made on tantalum and compared with available literature data. Tantalum was selected as a sample material for several reasons, key among these being our experiences with the material were extensive, the material is relatively inexpensive and its spectral emissivity is stable with repeated thermal cycling in vacuum.

Figure 14 represents the results of an observation of the spectral emissivity of tantalum at 1900K for the spectral region 2 to 11 μm. This graph is shown on the computer display unit screen; at the start of the observations, only the coordinate system appears and then as the readings are taken for each wavelength, dots appear representing the blackbody (H) and sample (S) signal levels. As the spectral emissivity for each wavelength is calculated, a solid line connecting the points is drawn, eventually giving the full emissivity spectra when the experiment is completed. At the upper left hand corner the temperature at the start (1933K) and completion (1935K) of the experiment are displayed. Other header type information has been removed for simplicity. This manner of displaying the emissivity spectra as the data is collected allows the operator to view the progress of the experiment and make any corrections that might be necessary.

The results for tantalum in two different experimental runs using two different tantalum samples are compared in Fig. 15. Both runs were performed at 1925K and in each case the tantalum tube was cleaned of surface impurities by heating under high vacuum to a temperature higher than that at which data was to be taken. The earlier data set shows a sharp

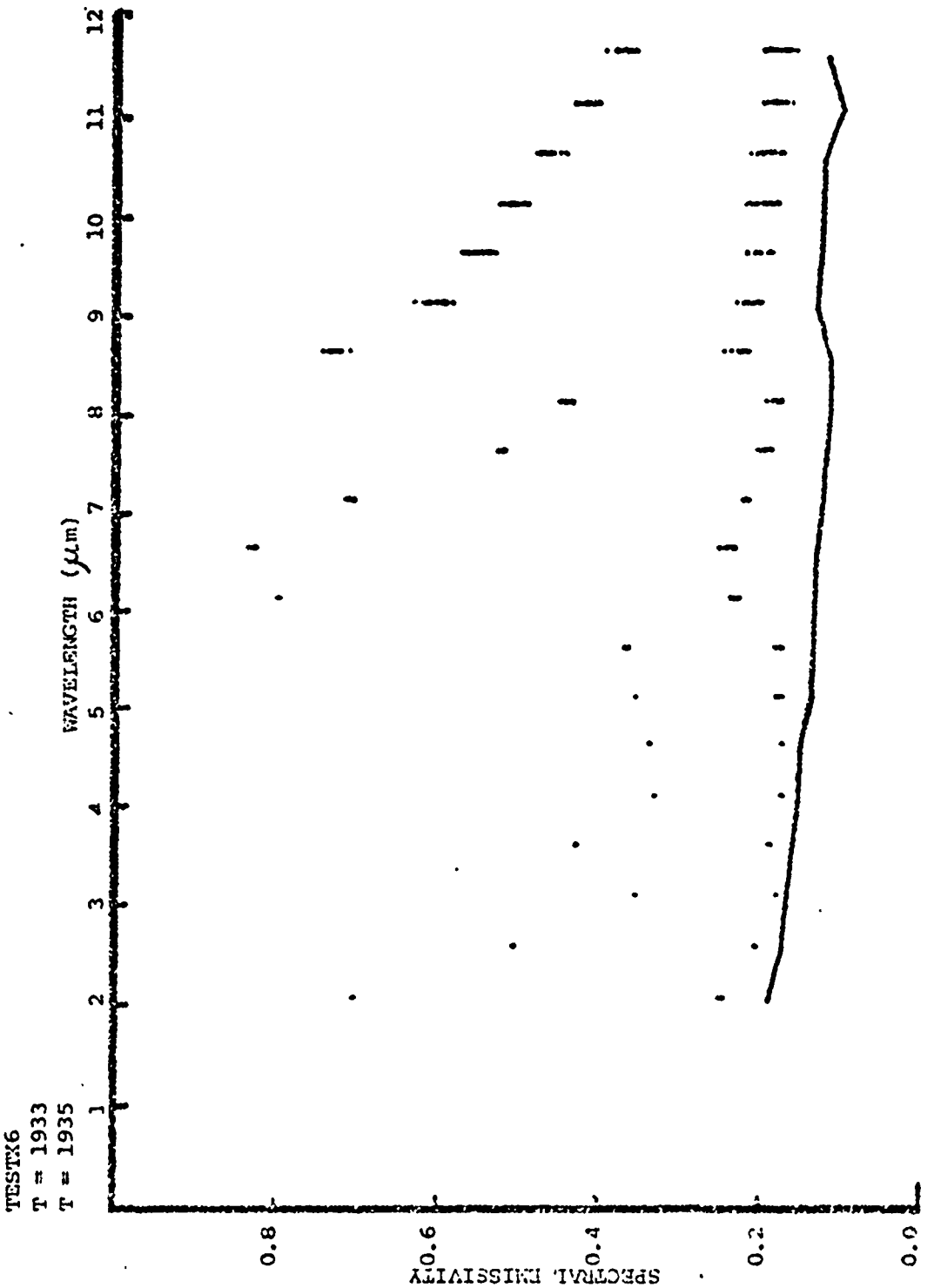

Figure 14. Typical emissivity spectra for tantalum as presented on the computer display during observations.

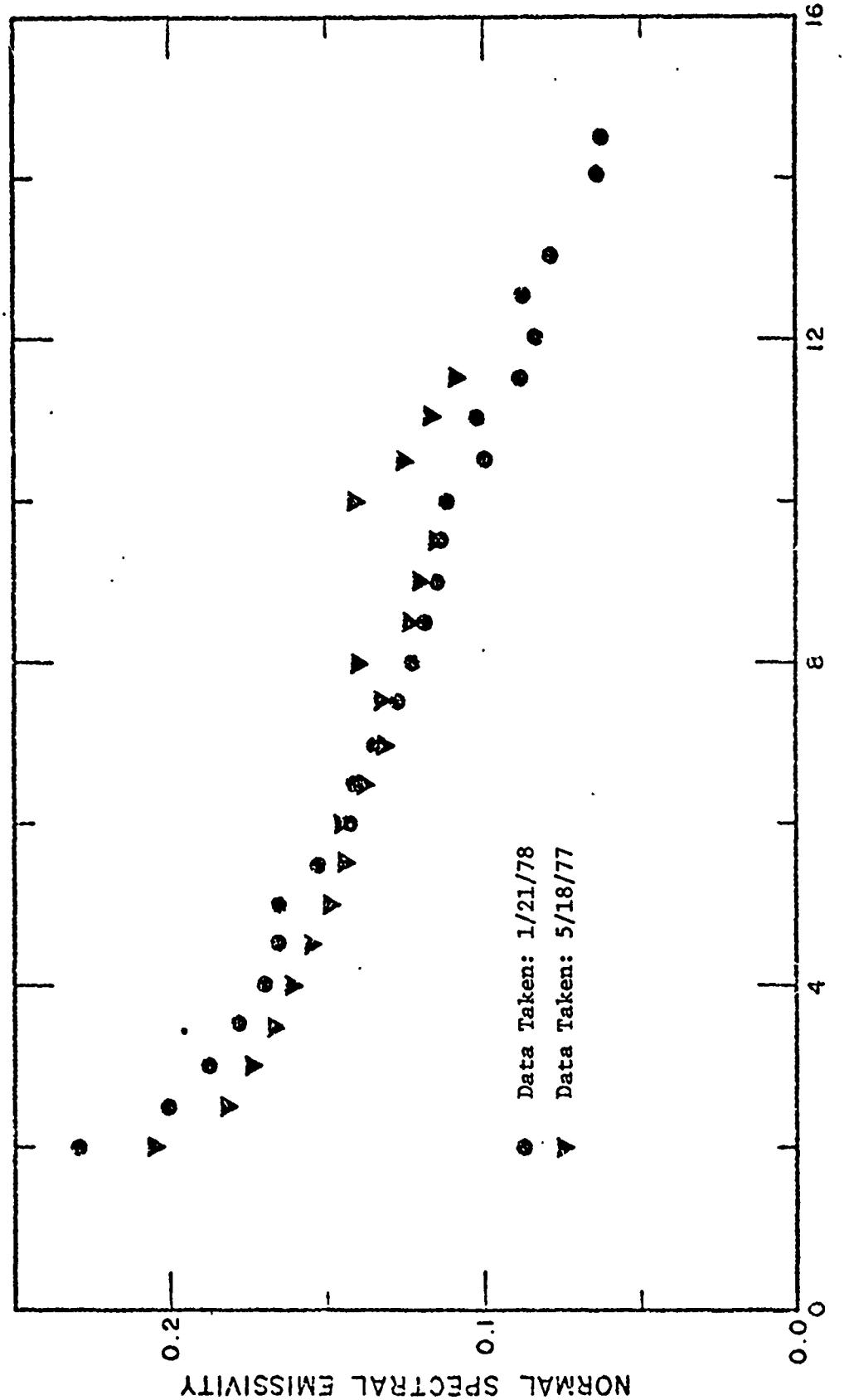

Figure 15. A comparison of two sets of tantalum spectral emissivity data.

increase in spectral emissivity at 10 μm. This increase is attributed to the sensitivity of the detector rather than an actual characteristic of the tantalum surface. Specifically, the emissometer was equipped with a thermal detector when this set of data was taken. The combination of the low detectivity of this detector and the small target size (0.8 mm dia) made it difficult to obtain signals with large signal-to-noise ratios beyond 9 μm. The second set of data, which does not display this increase at 10 μm, was obtained after the thermal detector had been replaced by the more sensitive, tri-metal photon detector. Neglecting all data above 9 μm reveals that the two sets of data are in good agreement. The apparent reproducibility of the results is an indication of the consistency of the performance of the emissometer over the nine month period between the collection of the first and second sets of data.

Comparison of the spectral emissivity results of our study at 1945K and 2286K with Riethof, et al [9,10,11] and with Kovalev and Muchnik [12] is made in Fig. 16. Much of the difference between our data and that of Riethof can be explained by surface conditions. Riethof reported that his tantalum spectral emissivity values were high (by 0.01 emittance unit) due to a surface film of an unidentified material which had formed on the measured sample surface. On the other hand, our tantalum surface was very well polished and oxide free and therefore lower spectral emissivity values would be expected.

The data of Kovalev and Muchnik at 1800K and 2200K are in excellent agreement with Riethof. Available sample characterization indicates the tantalum is of 98.8% purity and the vacuum conditions are not stated. Tabulated values are given in Appendix A for the measurements on tantalum presented in Figures 14 through 16.

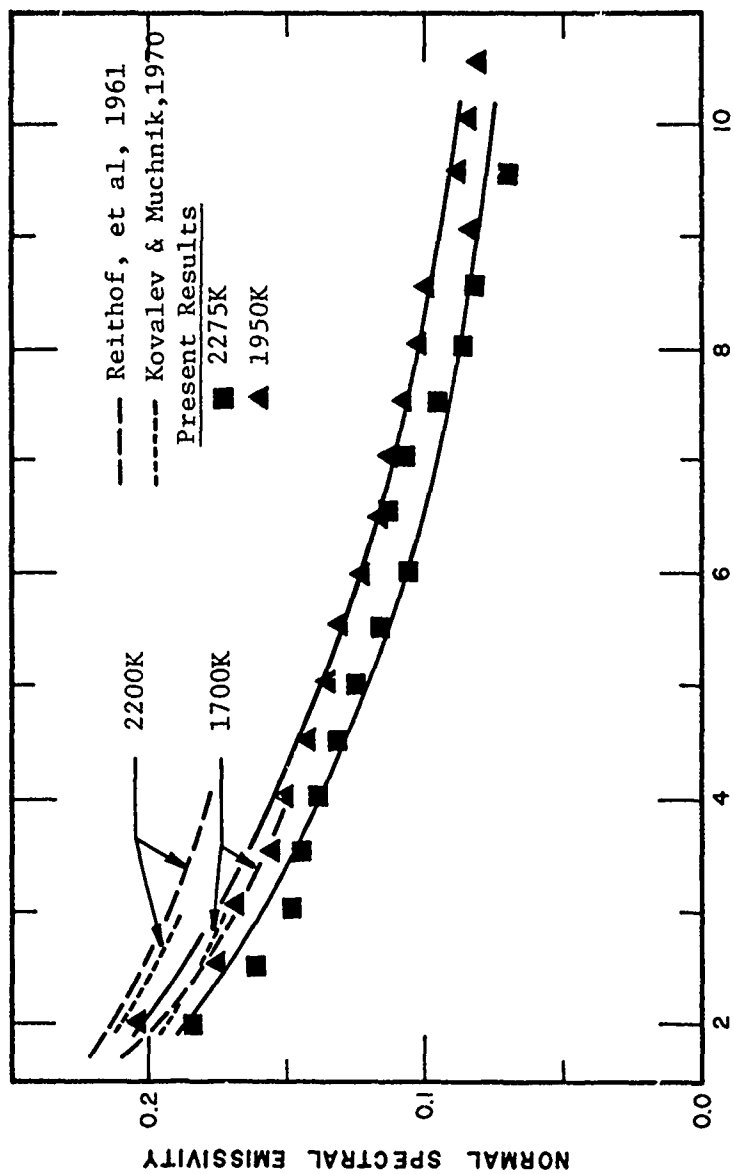

Figure 16. Spectral emissivity of tantalum compared to literature values.

GRAPHITE MEASUREMENTS AT HIGHER TEMPERATURES

In a separate study, the spectral emissivity of graphite was generated in the spectral region from 1 to 12 μm at a temperature of 2120K the results of which are presented in Figure 17. This is the first time graphite has ever been observed in the PRL emissometer and the first time that any sample has been tested at a temperature as high as 2120K. The data was very reproducible and the standard deviation in the spectral emissivity values were low compared with the deviation found when graphite was tested at lower temperatures. Low temperature poor performance is due to signal-to-noise problems with the thermocouple detector; since these measurements were made, the new trivalent metal detector has been installed with vastly improved performance.

For the results shown in Figure 17, the sample was in tubular form and heated directly. Unsuccessful attempts were made to measure the emissivity of a graphite cylindrical-shaped sample; that is, mounted within a tantalum heating tube. The resulting emissivity values were absurdly high-in the neighborhood of unity. We believe this is caused by contamination of the tantalum tube resulting in nonuniform temperatures in the blackbody and sample target regions of the tube. In earlier experiments with other materials, evidence of contamination was verified by changes in the resistivity of the heating tube measured at room temperature. It appears now that strict attention must be given to sample/heating tube interaction and probably it is best practice to use a heating tube with only one material and probably for only one experiment.

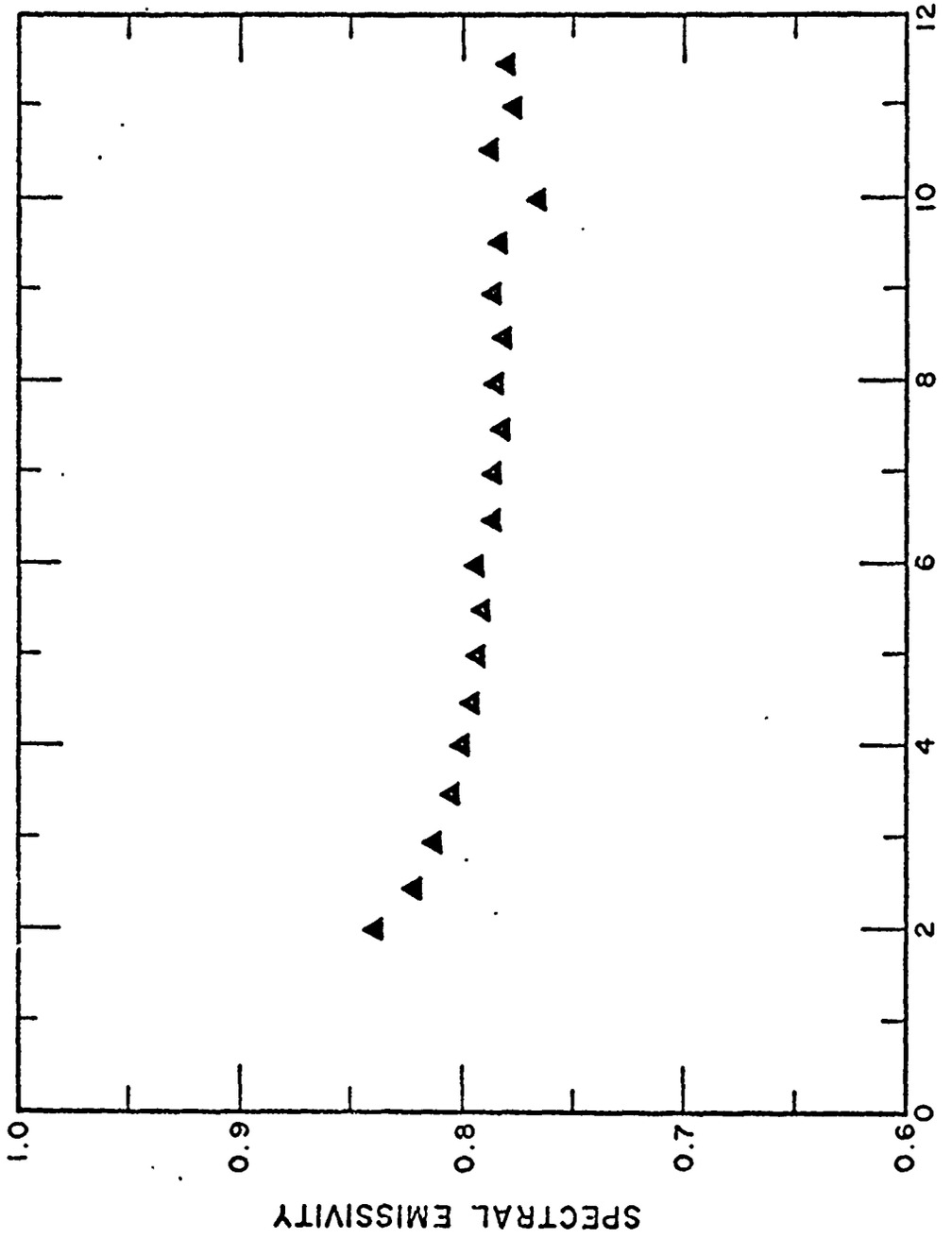

Figure 17. Spectral Emissivity of Graphite Sample (Directly Heated) at 2120 K.

PROPRIETARY GRAPHITE COMPOSITE STUDY

A brief study was undertaken to evaluate the feasibility of using the Multiproperty Apparatus for determining spectral emittance of a proprietary graphite composite material from the Naval Surface Weapons Center.

The available sample was a rectangular bar which was cut into two sections, hollowed out to form the blackbody cavity and placed back together. As shown in Figure 18, a round cross-section is machined at the ends to mate with extension tubes which engage the electrodes. In this configuration, the sample can be directly-electrically heated and the spectral emissivity measured by the emissometer. Using the voltage probes, as shown in Figure 18, permits calculation of the total emittance, ε_H, from the power dissipated in the test length and from the surface temperature.

Because the wall thickness of the sample cavity is relatively thick, there is an appreciable temperature difference, ΔT, between the surface and the inside of the cavity. The optical pyrometer (0.65 μm effective wavelength) sighting into the cavity opening indicates the "true" temperature of the cavity, T. The measured spectral radiance temperature, T_s, of the surface will be lower because the emissivity is less than unity and because of the wall ΔT. It is necessary to know the thermal conductivity in order to estimate ΔT which in turn allows correcting T_s. It is then possible to calculate the spectral emissivity, $\varepsilon_{0.65}$. The results of these observations are shown in Table 3 and Figure 19. Based upon our previous experiences, the corrections would increase the emmittance values about 25% at 0.65 μm and considerably less at longer wavelengths.

The normal spectral emittance values from 2 to 10.5 μm, obtained with the Emissometer, are plotted in Figure 20. The sample temperature was 1800K.

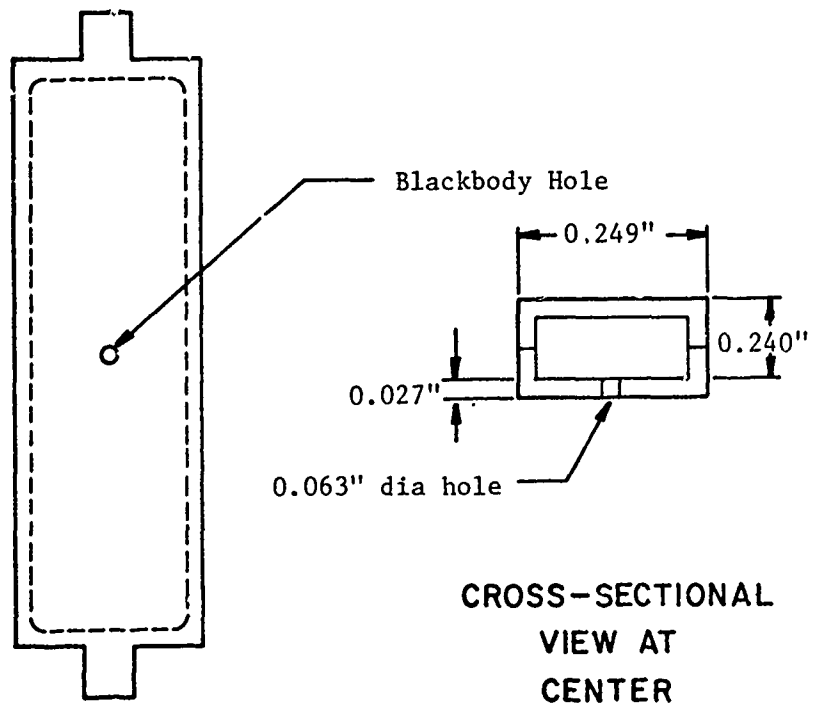

Figure 18. Sample configuration for the composite.

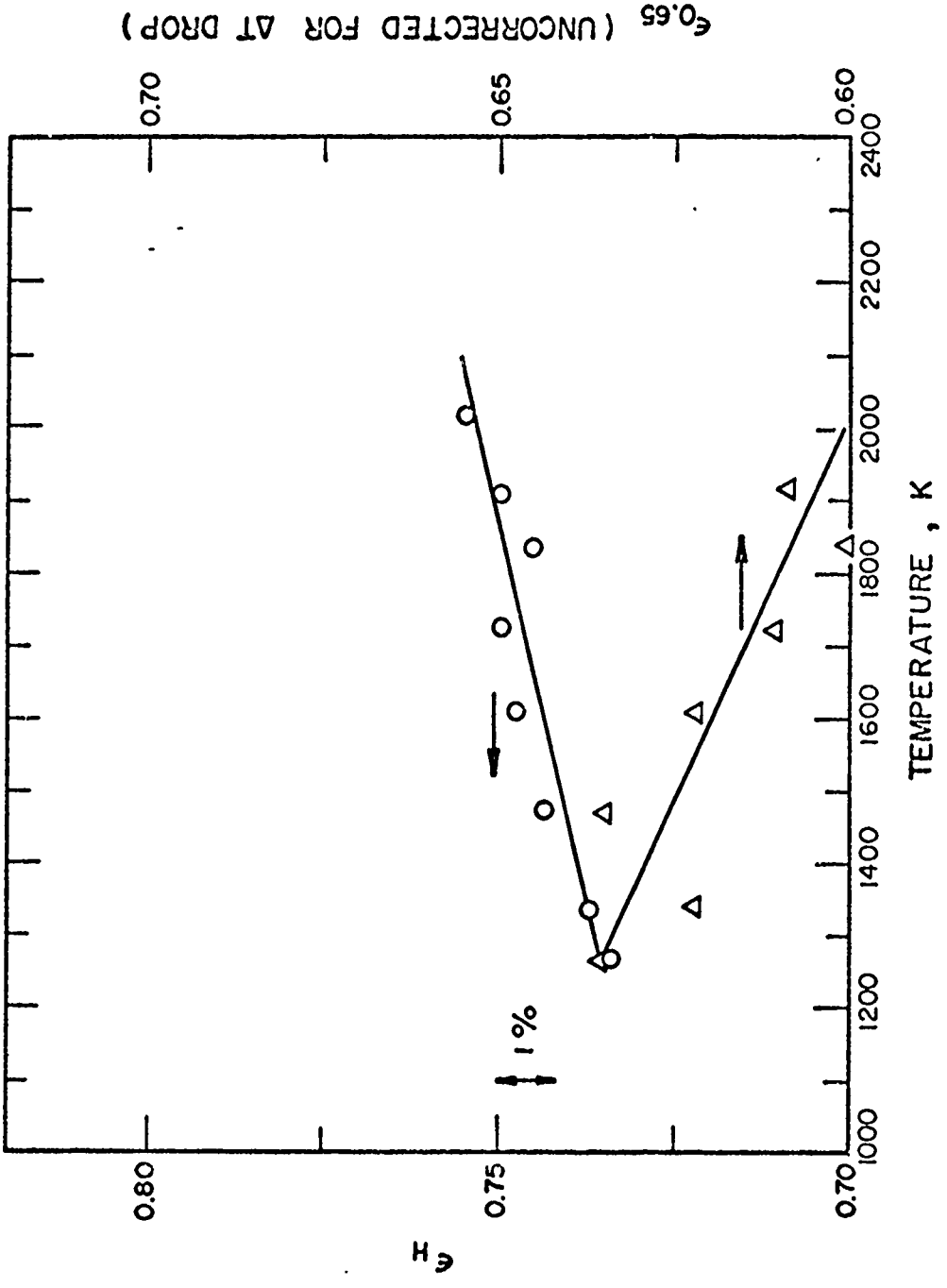

Figure 19. Total and Spectral Emittance (0.65 micrometers) as a Function of Temperature for the Graphite Composite.

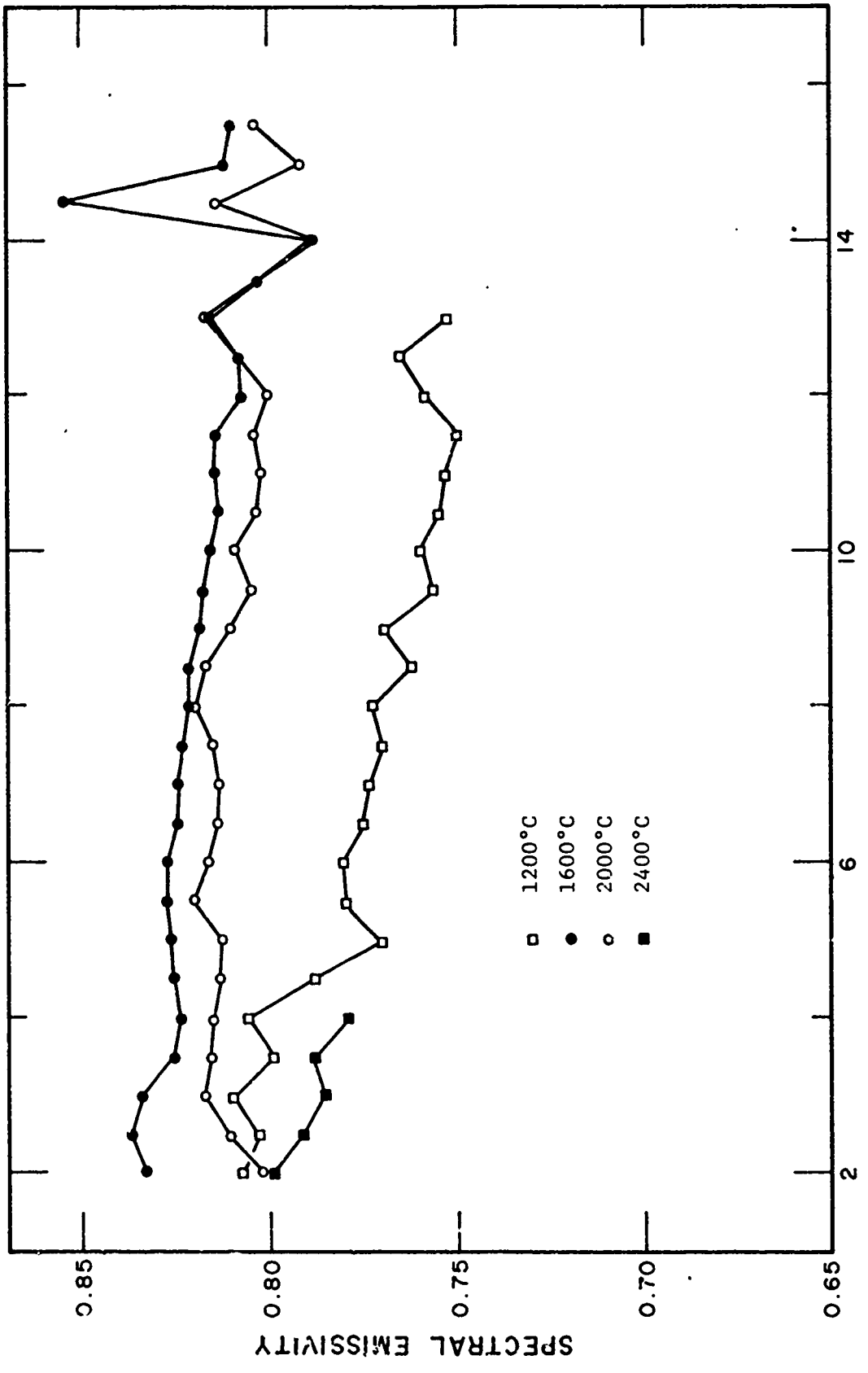

Figure 20. Spectral emissivity of the proprietary (NSWC) graphite composite sample.

Table 3

Hemispherical Total and Normal Spectral (0.65 μm) Emittance

Temp. (K)	ε_H	ε_λ(0.65 μm)*	T_s**
1260	0.733	0.636	1228.4
1338	0.737	0.622	1300.7
1474	0.743	0.635	1430.8
1609	0.747	0.621	1555.2
1726	0.749	0.610	1662.0
1838	0.745	0.601	1763.5
1908	0.750	0.609	1825.8
2006	0.755	-	-

* Uncorrected for temperature drop across the sample wall thickness.

** Spectral radiance temperature at 0.65 μm.

A correction for wall temperature ΔT is also needed for these data. This correction is less than for $\varepsilon_{0.65}$ but it has not been determined. The results obtained during several preliminary (setting up) runs are included. The results are within a few percent of each other. The spectral emittance decreases with increasing wavelength. An extrapolation of this data to 0.65 micrometers would yield a result of about 0.77 which is about 21 percent higher than the uncorrected value of 0.61 (Table 3 and Figure 19) obtained for $\varepsilon_{0.65}$ with the pyrometer. This is in line with previous observations which predict about a +25% correction for the pyrometer data, and assuming that the correction for the emissometer data is much smaller.

Additional study is required to evaluate the effect of temperature drop due to the finite wall thickness of the sample cavity. We expect that some funding will be made available from the NSWC to pursue this new technique for measurements on composites.

CERAMIC SAMPLE MEASUREMENTS

Sample Descriptions

Samples of silicon carbide were obtained from Carborundum, Ceradyne and General Electric. Samples of silicon nitride were obtained from Airesearch, Kawecki-Berylco and Kyocera. Samples were also obtained from Norton Company but because of machining difficulties were not included in the present measurement program. The addresses of the suppliers are given in Appendix B. Sample descriptions are given in Table 4.

The Carborundum silicon carbide samples were formed by cold pressing silicon carbide powder and then sintering the material at temperatures in excess of 2000°C. The final cylindrical sample was obtained by diamond grinding. The sample was reported as being 99% silicon carbide with the remainder being composed primarily of sintering aide, boron and carbon.

Two types of silicon carbide were obtained from Ceradyne: Ceralloy 146A and Ceralloy 146I. Both types are prepared by hot-pressing. The final sample shape was formed by diamond grinding. Each type of sample was reported as having no free silicon or carbon. Ceralloy 146A is composed of about 98% silicon carbide and 2% Al_2O_3, with traces of tungsten present. Ceralloy 146I was 98% silicon carbide and 2% boron carbide.

The silicon carbide sample supplied by General Electric was prepared by cold-pressing submicron β silicon carbide power at 4000 psi and sintering for 30 minutes at 2060°C in vacuum. The resulting material was diamond ground to the appropriate diameter.

The Airesearch silicon nitride samples were reaction-bonded. Silicon powder was slip cast in a nitrogen atmosphere. Small amounts of iron were added to this process to aid in converting silicon to silicon nitride.

Table 4

Description of the Ceramic Samples

Manufacturer	Major Constituent	Designation	Phase	Density (g/cm^3)	Major Impurities	Grain Size (μm)	Process
Carborundum	SiC		α	3.15	1% B+C	7	Cold Press & Sinter
Ceradyne	SiC	Ceralloy 146A	α	3.30	2% Al_2O_3	5-10	Hot-Press
Ceradyne	SiC	Ceralloy 146I	α	3.00	2% B_4C	coarse	Hot-Press
General Electric	SiC		β	3.00	W Trace 0.8% B+C	3-5	Cold Press & Sinter
Airesearch	Si_3N_4		$\alpha+\beta$	2.75	1% Fe	5-10	Reaction Bonded
Kawecki-Berylco	Si_3N_4		70-80% α 30-70% β	2.38	3/4% Si	2-4	Reaction Bonded
Kyocera	Si_3N_4			2.70	1% Al_2O_3		Cold Press & Sinter

The final iron content was estimated at being 1%. The sample was made up of a mixture of α and β phases. The measured surface was as-received and no diamond grinding was employed to obtain final dimensions.

A reaction-bonded silicon nitride sample was supplied by Kawecki-Berylco. This sample was prepared from silicon powder but no iron was added at a nitriding aid. The final sample shape was obtained by diamond grinding. The sample was reported to be 70 to 80% α phase (hexagonal), with the remainder as β phase. Residual free silicon (1/2 to 1%) was present.

The Kyocera silicon nitride sample (SN205) was prepared by cold pressing silicon nitride powder and then sintering at temperatures in excess 1600°C. The sample form was obtained by diamond grinding the rough form produced by cold pressing. The sample was reported as being about 99% pure silicon nitride and 1% Al_2O_3.

Spectral Emissivity Results - Silicon Carbide

The normal spectral emissivity data of SiC for each sample was measured (after a 10 minute pretreatment at 1950K in high vacuum) first at 1900K, then at 1800K, and in one case at 1700K. The data obtained at 1900K are given in Table 5. Repeat measurements were made on each of the four samples and these data are also included in this table. The data for the first run on the Carborundum and the Ceralloy 146A samples and the data for the repeat run on the Ceralloy 146I and General Electric samples are plotted in Fig. 21. From this figure, it can be seen that the spectral emissivity of Ceralloy 146A has no structure, that the emissivity data of the Ceralloy 146I and Carborundum samples exhibit a small peak at about 11 μm and a large valley near 12.5-13 μm, and the emissivity of the

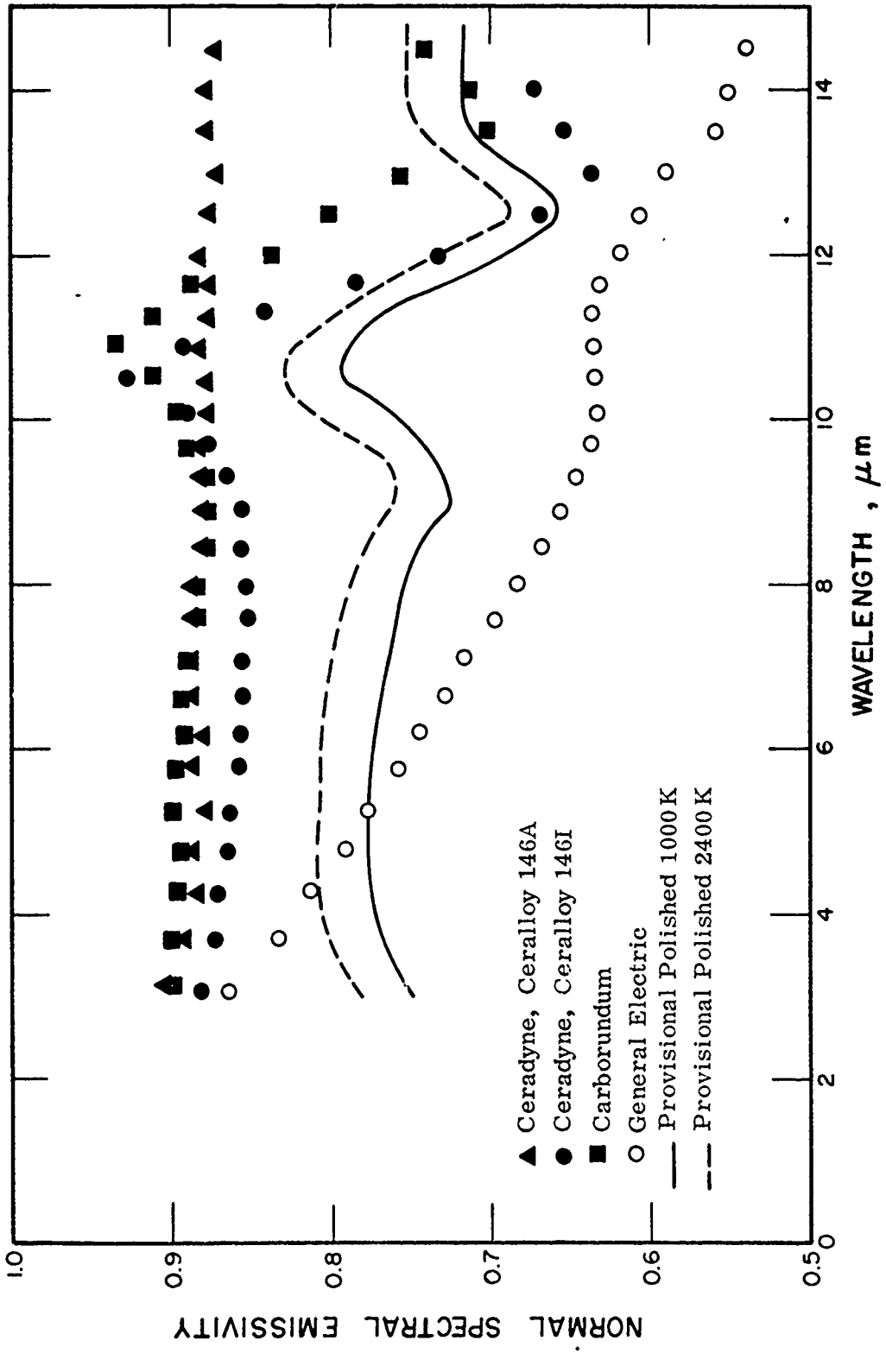

Figure 21. Normal Spectral Emissivity of Silicon Carbide at 1900 K.

Table 5

Normal Spectral Emissivity of Silicon Carbide at 1900K

Wavelength (μm)	Sample/Trial: Carborundum First	Carborundum Repeat	Ceralloy 146A First	Ceralloy 146A Repeat	Ceralloy 146I First	Ceralloy 146I Repeat	G.E. Co. First	G.E. Co. Repeat
3.25	0.903	0.908	0.904	0.905	0.875	0.881	0.856	0.865
3.75	0.905	0.905	0.890	0.894	0.870	0.875	0.822	0.834
4.25	0.903	0.907	0.885	0.885	0.865	0.871	0.802	0.812
4.75	0.899	0.904	0.885	0.886	0.859	0.865	0.780	0.791
5.25	0.895	0.906	0.879	0.880	0.861	0.865	0.765	0.776
5.75	0.901	0.911	0.889	0.893	0.858	0.859	0.751	0.759
6.20	0.896	0.908	0.882	0.887	0.857	0.857	0.733	0.743
6/65	0.893	0.907	0.887	0.886	0.857	0.855	0.717	0.727
7.10	0.891	0.908	0.887	0.888	0.855	0.856	0.702	0.712
7.60	0.889	0.906	0.885	0.889	0.857	0.851	0.687	0.697
8.00	0.885	0.906	0.888	0.880	0.858	0.854	0.672	0.681
8.50	0.886	0.909	0.884	0.883	0.860	0.856	0.658	0.668
8.90	0.883	0.906	0.880	0.884	0.864	0.856	0.648	0.655
9.30	0.880	0.911	0.883	0.884	0.872	0.866	0.640	0.646
9.75	0.884	0.908	0.884	0.883	0.891	0.878	0.634	0.638
10.1	0.890	0.913	0.879	0.884	0.910	0.897	0.652	0.634
10.5	0.912	0.923	0.878	0.882	0.932	0.923	0.631	0.635
10.9	0.934	0.930	0.881	0.891	0.887	0.892	0.634	0.635
11.3	0.912	0.923	0.879	0.885	0.812	0.839	0.632	0.637
11.7	0.887	0.906	0.879	0.888	0.752	0.784	0.624	0.630
12.1	0.837	0.891	0.883	0.882	0.675	0.732		0.618
12.5	0.802	0.871	0.876		0.633	0.667		0.604
13.0	0.756	0.851	0.872		0.588	0.635		0.589
13.5	0.702	0.819	0.878		0.591	0.655		0.558
14.0	0.715	0.807	0.877		0.651	0.672		0.551
14.5	0.742	0.828	0.874					0.537
15.0	0.763	0.835	0.857					

General Electric samples decreases strongly with increasing wavelength from 2 to 14.5 μm except for a plateau near 11 μm. An examination of the data (Table 5) shows that the results were reproducible to generally better than 1% except for the Carborundum and Ceralloy 146I samples in the spectral regions where there is spectral character.

The emissivity data for SiC at 1800K are given in Table 6. These data are very similar to the results obtained at 1900K but are generally slightly higher. A comparison of the 1800 and 1900K data for the Carborundum sample is given in Fig. 22, for the Ceralloy 146A sample in Fig. 23, for the Ceralloy 146I sample in Fig. 24, and for the General Electric sample in Fig. 25. Table 7 gives the data for the temperature dependency of the Ceralloy 146A sample.

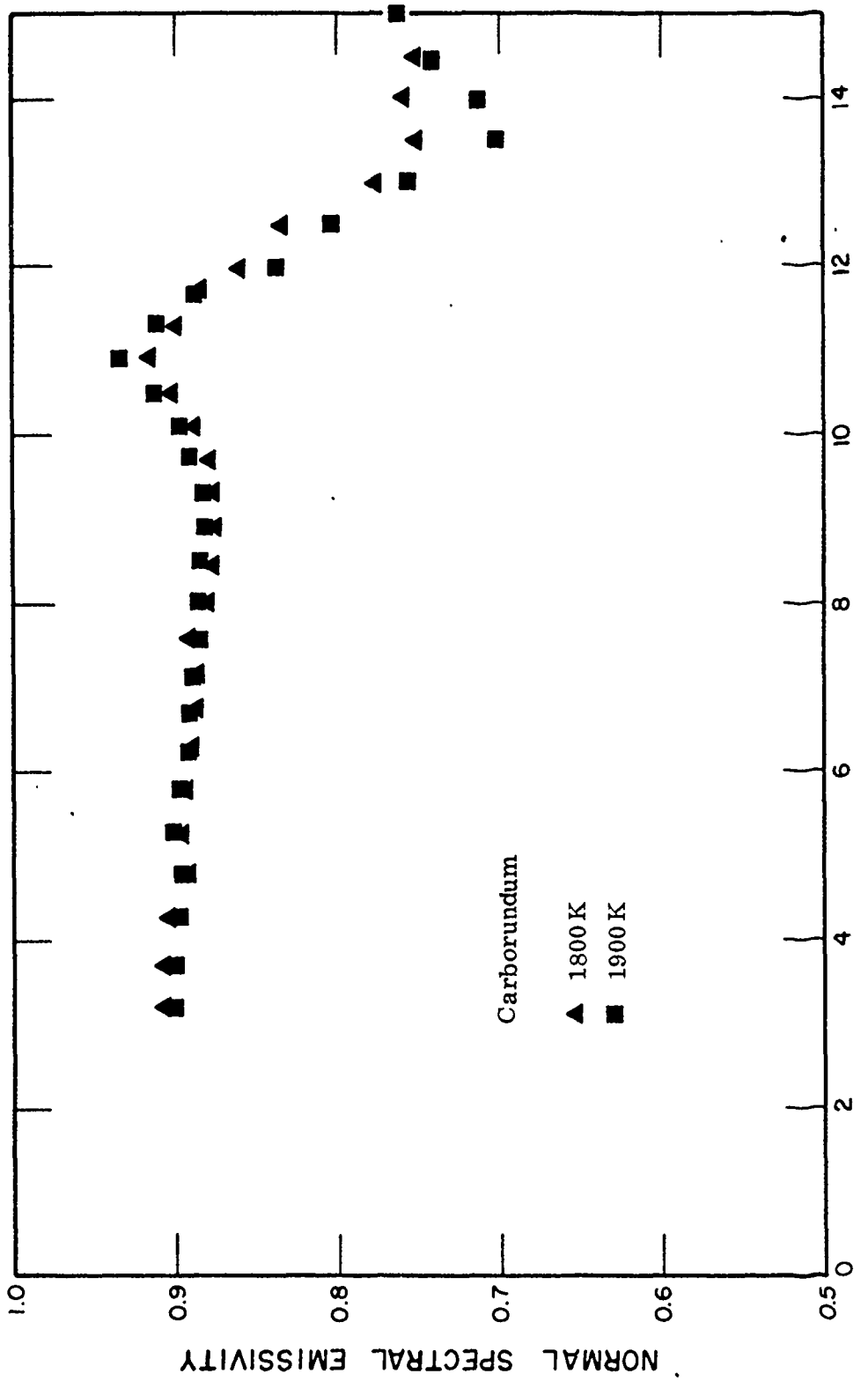

Figure 22. Normal Spectral Emissivity of Silicon Carbide Obtained from Carborundum.

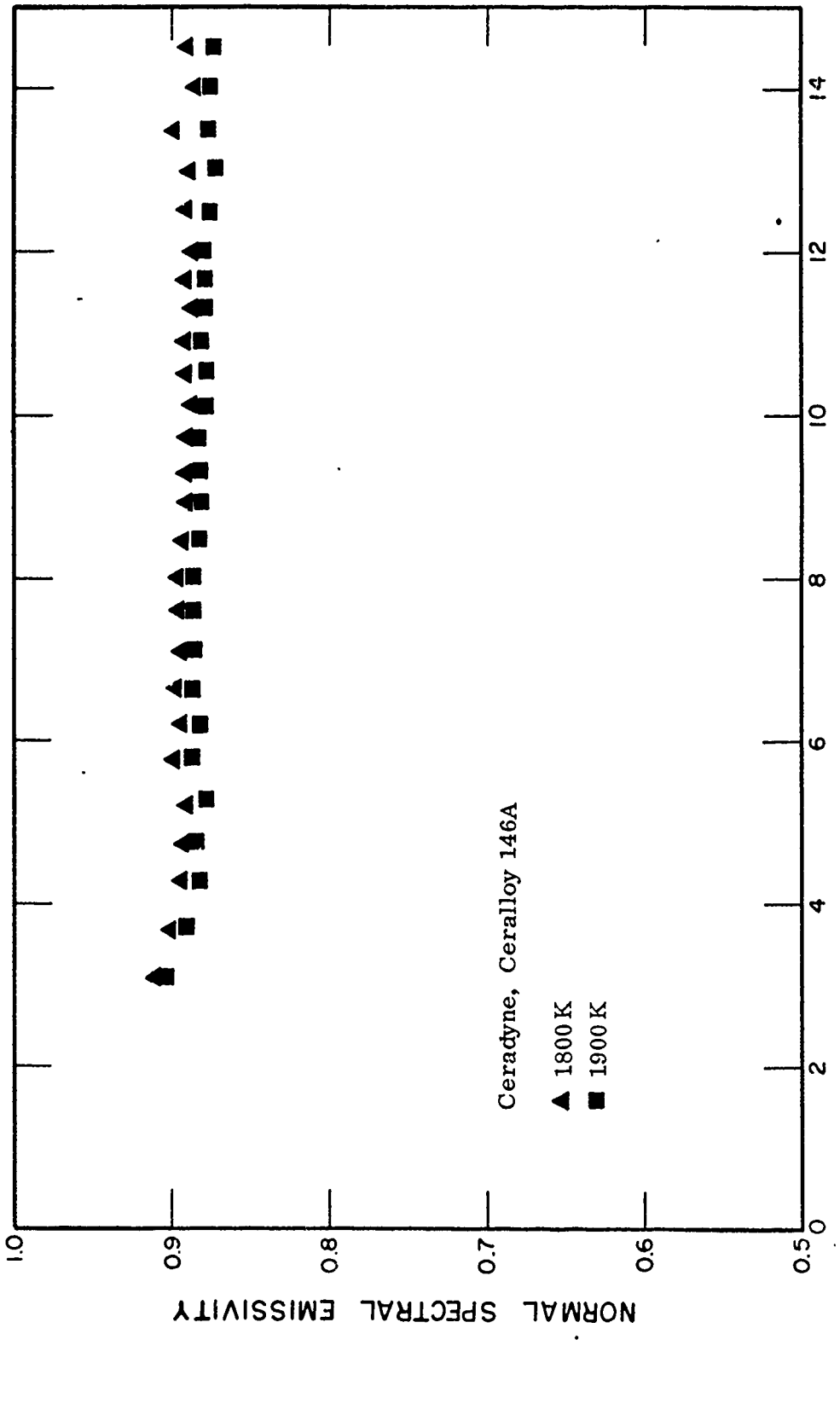

Figure 23. Normal Spectral Emissivity of Silicon Carbide Obtained from Ceradyne (Ceralloy 146A).

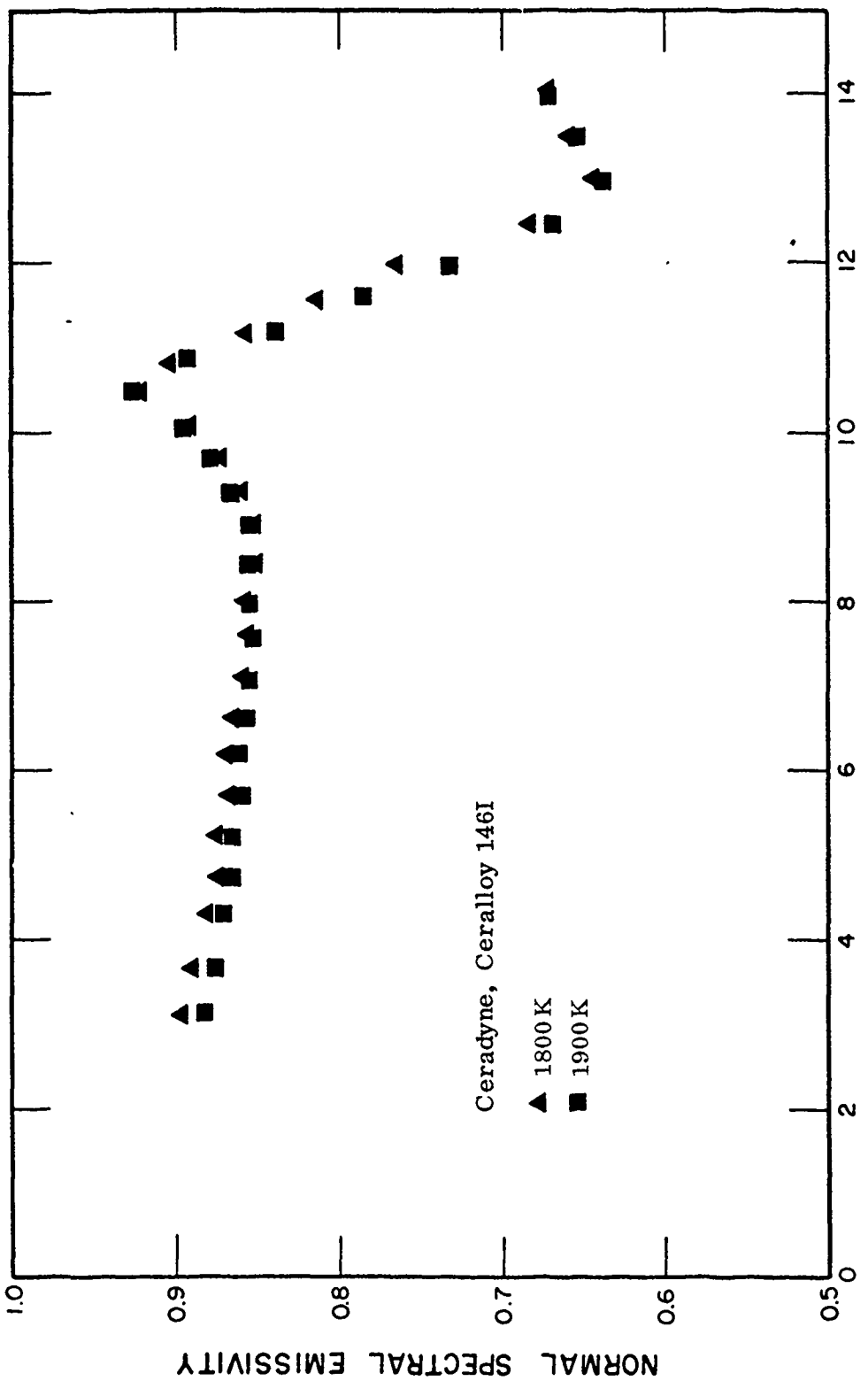

Figure 24. Normal Spectral Emissivity of Silicon Carbide Obtained from Ceradyne (Ceralloy 146I).

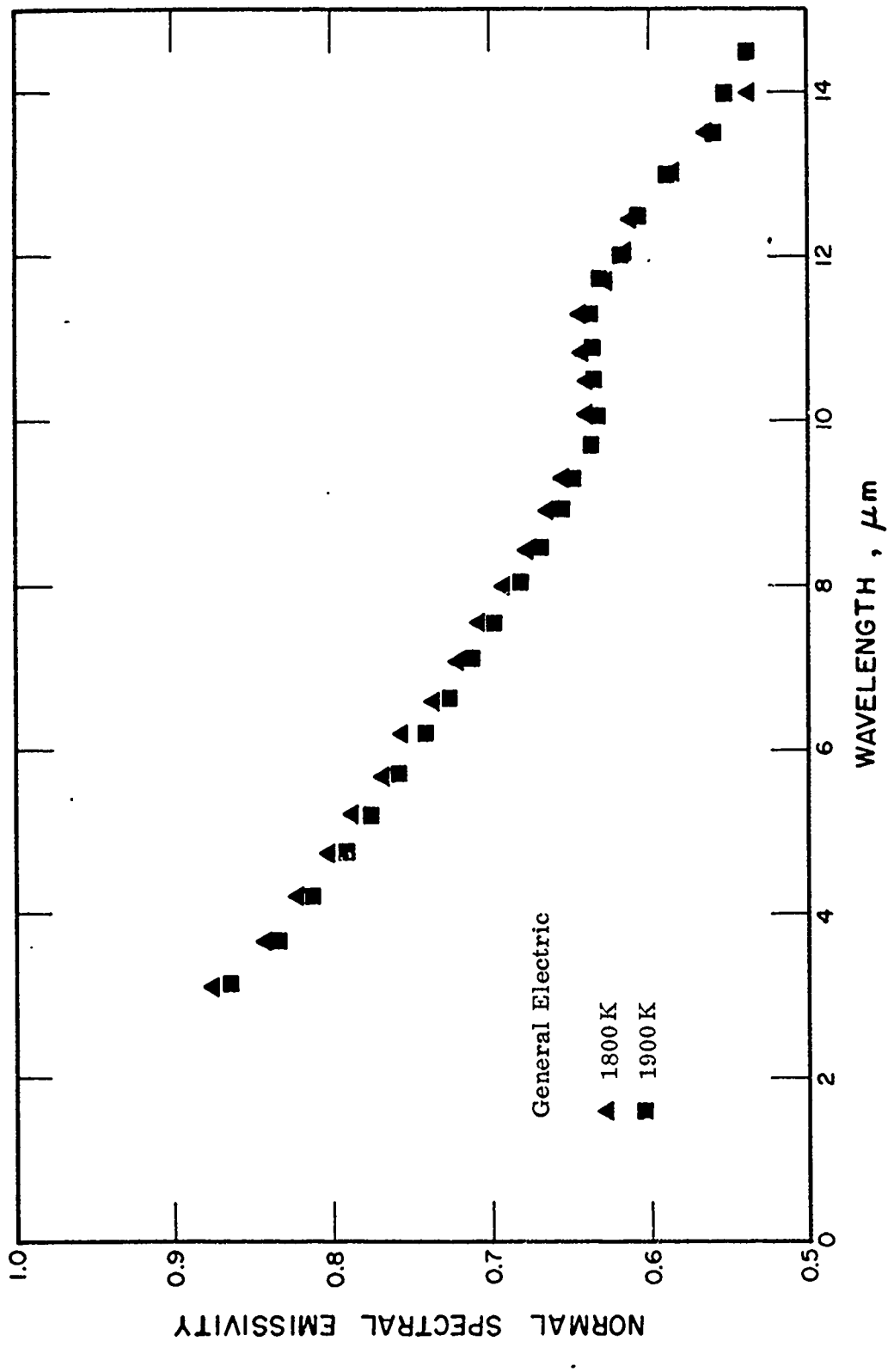

Figure 25. Normal Spectral Emissivity of Silicon Carbide Obtained from General Electric.

Table 6

Normal Spectral Emissivity of Silicon Carbide at 1800K

Wavelength (μm)	Sample/Trial: Carborundum	Ceralloy 146A First	Ceralloy 146A Repeat	Ceralloy 146I First	Ceralloy 146I Repeat	G.E. Co.
3.25	0.907	0.912	0.913	0.899		0.873
3.75	0.903	0.902	0.903	0.890		0.845
4.25	0.901	0.895	0.897	0.881		0.822
4.75	0.893	0.895	0.894	0.874		0.803
5.25	0.896	0.892	0.896	0.874		0.790
5.75	0.896	0.900	0.901	0.868		0.771
6.20	0.891	0.894	0.899	0.867		0.757
6.65	0.888	0.898	0.902	0.861		0.738
7.10	0.886	0.895	0.900	0.855		0.720
7.60	0.887	0.896	0.900	0.854		0.708
8.00	0.881	0.896	0.903	0.853		0.693
8.50	0.879	0.893	0.906	0.852		0.676
8.90	0.879	0.891	0.898	0.857		0.665
9.30	0.880	0.892	0.899	0.860		0.655
9.75	0.879	0.890	0.899	0.871		0.647
10.1	0.889	0.890	0.895	0.895	0.899	0.640
10.5	0.905	0.894	0.899	0.924	0.927	0.638
10.9	0.915	0.894	0.902	0.901	0.908	0.639
11.3	0.900	0.889	0.905	0.857	0.862	0.637
11.7	0.888	0.893	0.903	0.816	0.813	0.627
12.1	0.862	0.886	0.908	0.768		0.620
12.5	0.835	0.893		0.683		0.609
13.0	0.779	0.890		0.642		0.584
13.5	0.753	0.901		0.655		0.561
14.0	0.760	0.884		0.678		0.535
14.5	0.752	0.893				
15.0						

Table 7

Temperature Dependency of Normal Spectral Emissivity of SiC (Ceralloy 146A)

Wavelength (μm)	Temperature, K					
	1700K	1700K	1800K	1800K	1900K	1900K
3.25	0.907	0.904	0.912	0.913	0.904	0.905
3.75	0.895	0.894	0.902	0.903	0.890	0.894
4.25	0.889	0.891	0.895	0.897	0.885	0.885
4.75	0.890	0.891	0.895	0.894	0.885	0.886
5.25	0.885	0.888	0.892	0.896	0.879	0.879
5.75	0.897	0.898	0.900	0.901	0.889	0.893
6.20	0.895	0.895	0.894	0.899	0.882	0.887
6.65	0.896	0.898	0.898	0.902	0.887	0.886
7.10	0.895	0.897	0.895	0.900	0.887	0.888
7.60	0.898	0.898	0.896	0.900	0.885	0.889
8.00	0.897	0.897	0.896	0.903	0.888	0.880
8.50	0.896	0.898	0.893	0.906	0.884	0.883
8.90	0.894	0.898	0.891	0.898	0.880	0.884
9.30	0.898	0.896	0.892	0.899	0.882	0.884
9.75	0.894	0.897	0.890	0.899	0.884	0.883
10.1	0.895	0.903	0.890	0.895	0.879	0.884
10.5	0.895	0.897	0.894	0.899	0.878	0.882
10.9	0.894	0.902	0.893	0.902	0.881	0.891
11.3	0.900	0.902	0.889	0.905	0.879	0.885
11.7	0.908	0.897	0.893	0.903	0.879	0.888
12.1	0.910	0.886	0.886	0.908	0.883	0.882
12.5		0.899	0.893		0.876	
13.0		0.909	0.890		0.872	
13.5		0.903	0.901		0.878	
14.0		0.880	0.884		0.877	
14.5		0.916	0.893		0.874	
					0.857	

Spectral Emissivity Results - Silicon Nitride

Because of the instability of silicon nitride at high temperatures under vacuum, emissivity data were first taken at 1600K, then 1700K and in some cases at 1800K. Emissivity values changed rapidly at 1800K. Data at 1700K for samples from the three manufacturers are shown in Fig. 26 and are given in Table 8. The data all show an increase in emissivity from 3 to 8 μm, a decrease from 8 to 11 μm and an increase in the 11 to 14 μm. The data obtained at 1600K are given in Table 9. These data show the reproducibility of the data to be at 1600K to be generally better than 1% over the entire wavelength region. However, the data are not reproducible at 1800K. The results continued to change at 1800K during the measurements. Table 10 gives the data for four runs on the Airesearch sample and two runs on the Kyocera sample. These data show that the emissivity values changed markedly for silicon nitride at 1800K under high vacuum. Results for the Airesearch sample at 1600, 1700 and 1800K are shown in Fig. 27. Results for the Kawecki-Berylco sample at 1600 and 1700K are given in Fig. 28 and results for the Kyocera sample at 1600, 1700 and 1800K are given in Fig. 29.

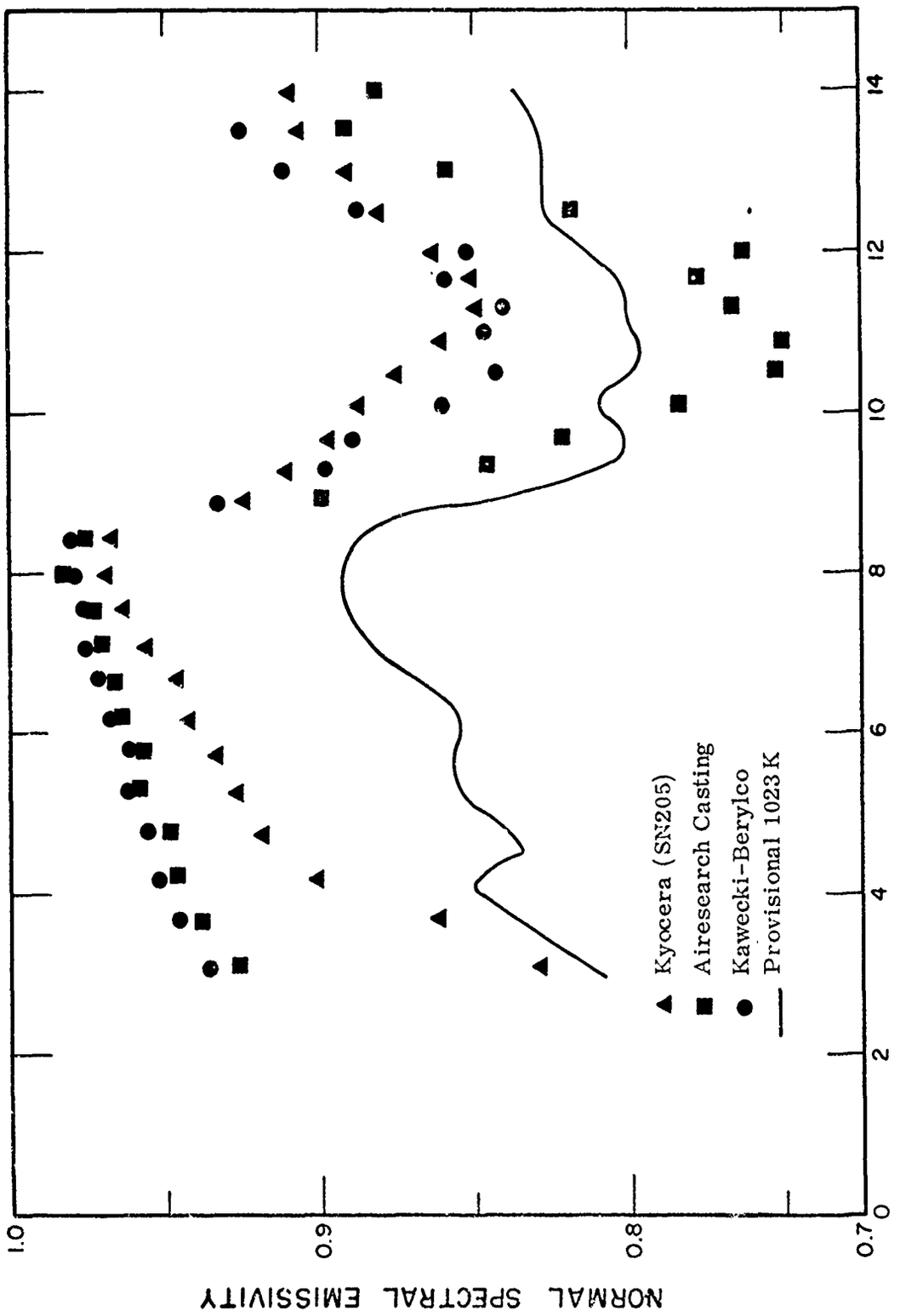

Figure 26. Normal Spectral Emissivity of Silicon Nitride at 1700 K.

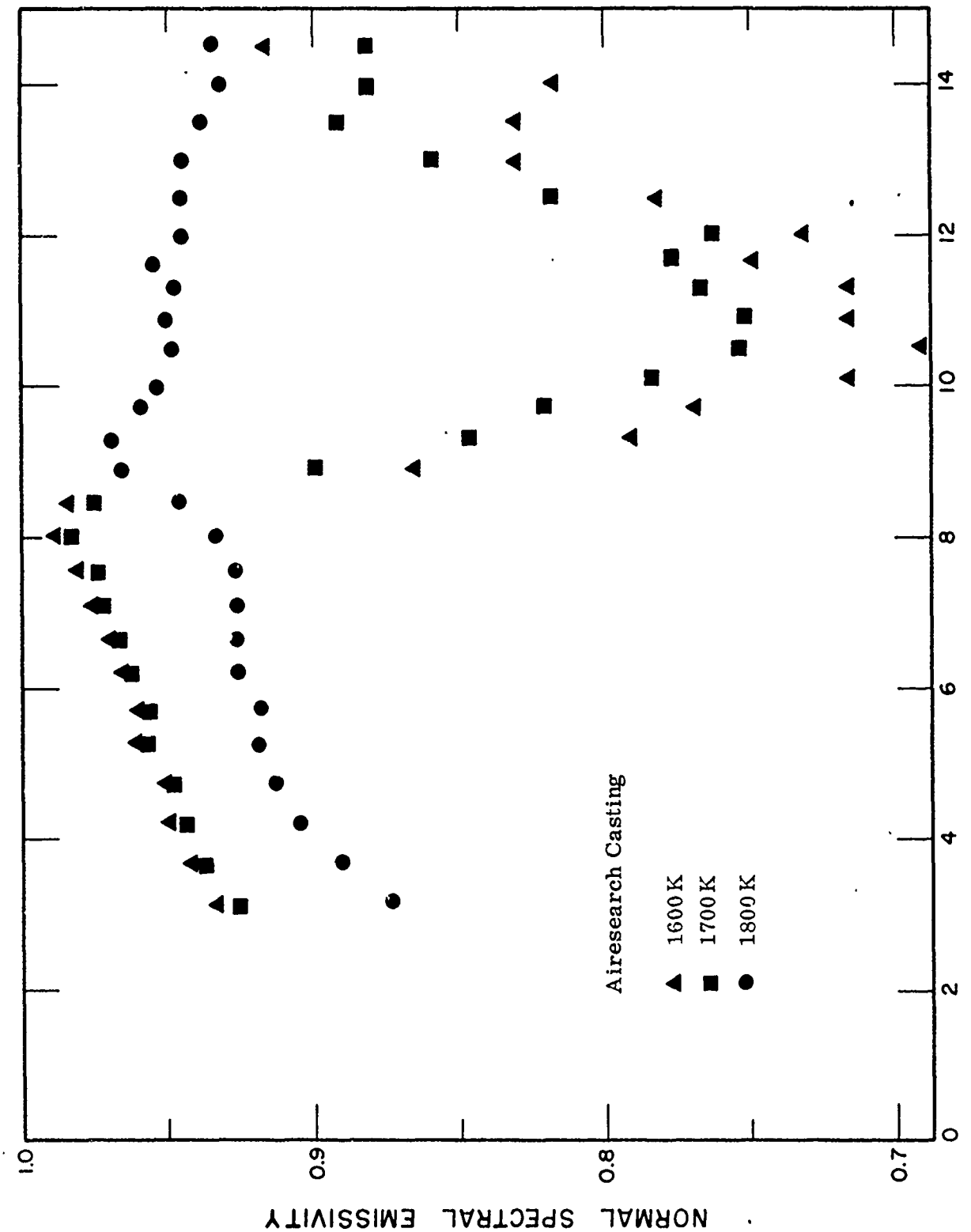

Figure 27. Normal Spectral Emissivity of Silicon Nitride Obtained from Airesearch.

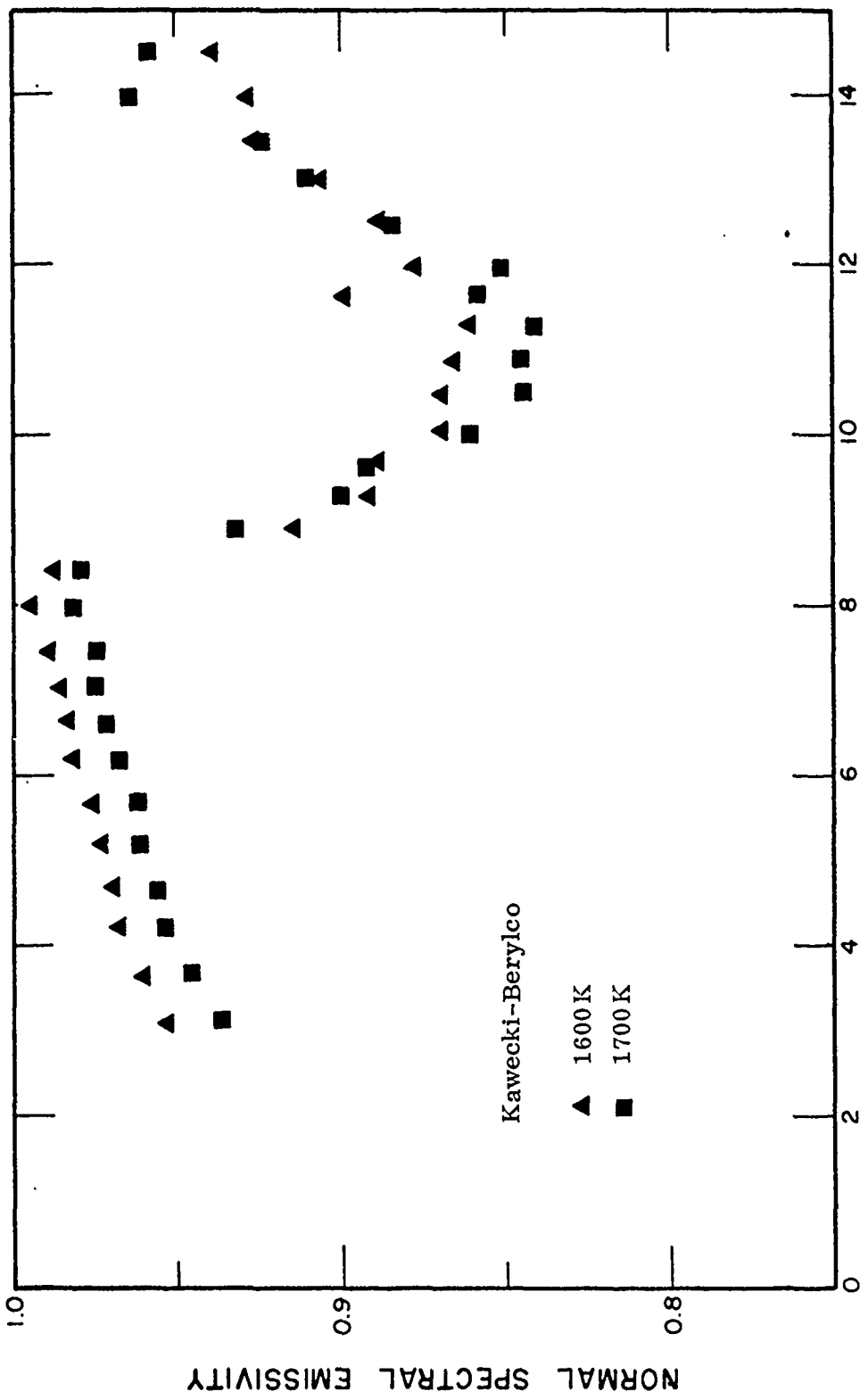

Figure 28. Normal Spectral Emissivity of Silicon Nitride Obtained from Kawecki-Berylco.

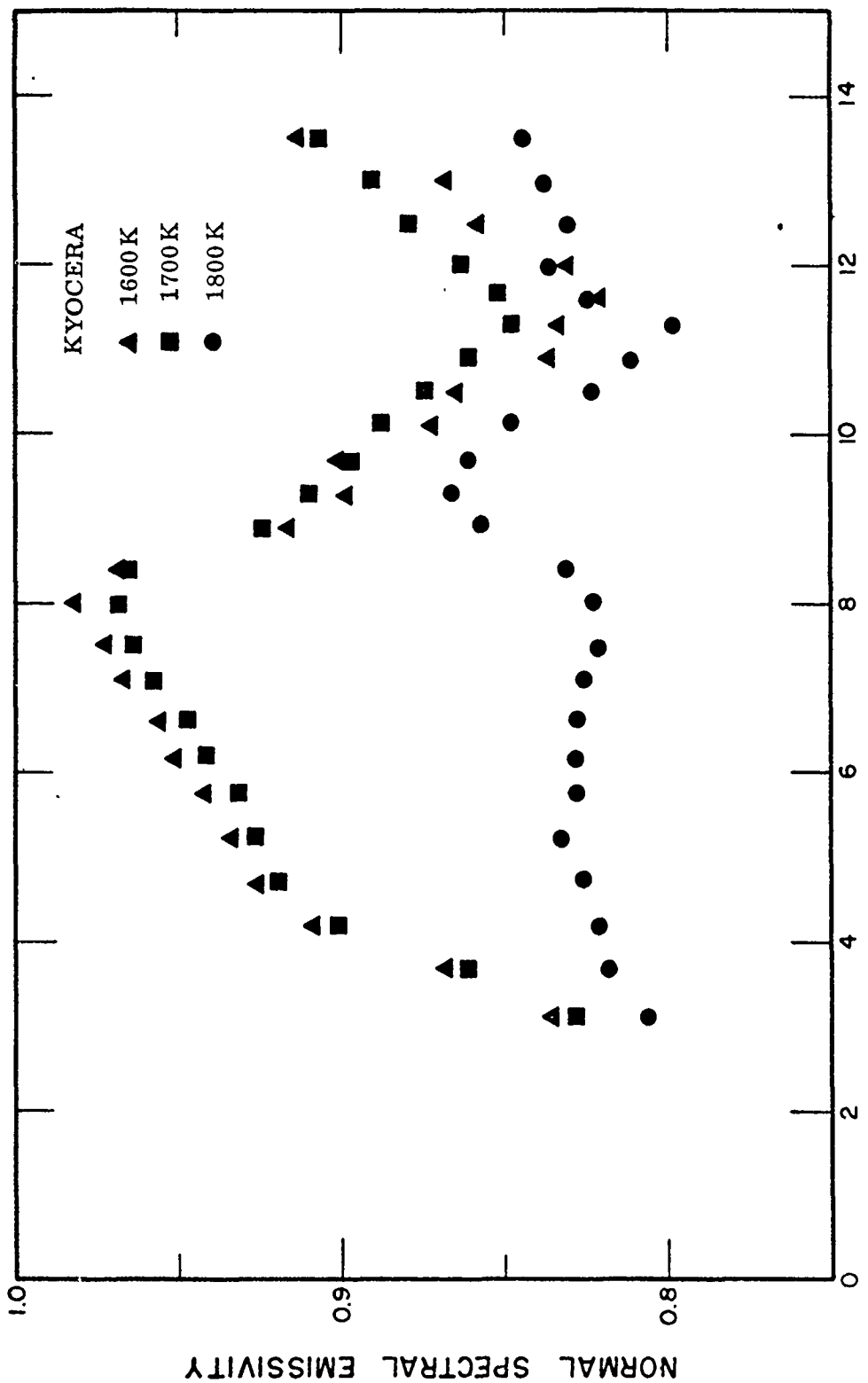

Figure 29. Normal Spectral Emissivity of Silicon Nitride Obtained from Kyocera.

Table 8

Normal Spectral Emissivity of Silicon Nitride at 1700K

Wavelength (μm)	Sample/Trial: Airesearch First	Airesearch Repeat	Kawecki-Berylco	Kyocera
3.25	0.927	0.923	0.937	0.830
3.75	0.939	0.935	0.946	0.862
4.25	0.945	0.943	0.952	0.900
4.75	0.950	0.949	0.956	0.919
5.25	0.958	0.952	0.962	0.927
5.75	0.957	0.953	0.962	0.934
6.20	0.963	0.954	0.968	0.942
6.65	0.967	0.955	0.972	0.947
7.10	0.971		0.975	0.957
7.60	0.974		0.974	0.964
8.00	0.984		0.980	0.968
8.50	0.975		0.978	0.967
8.90	0.899		0.932	0.925
9.30	0.846		0.899	0.910
9.75	0.821		0.890	0.907
10.1	0.784		0.860	0.888
10.5	0.754		0.843	0.875
10.9	0.750		0.846	0.860
11.3	0.767		0.840	0.848
11.7	0.777		0.859	0.851
12.1	0.762		0.852	0.864
12.5	0.819		0.888	0.880
13.0	0.858		0.912	0.891
13.5	0.892		0.925	0.907
14.0	0.881		0.965	0.909
14.5	0.882		0.959	

Table 9

Normal Spectral Emissivity of Silicon Nitride at 1600K

Wavelength (μm)	Sample/Trial: Airesearch First	Airesearch Repeat	Kawecki-Berylco First	Kawecki-Berylco Repeat	Kyocera First	Kyocera Repeat
3.25	0.935	0.937	0.960	0.953	0.842	0.837
3.75	0.942	0.936	0.968	0.960	0.869	0.870
4.25	0.950	0.942	0.973	0.966	0.908	0.909
4.75	0.952	0.948	0.976	0.969	0.925	0.927
5.25	0.960	0.955	0.979	0.973	0.933	0.934
5.75	0.961	0.955	0.979	0.975	0.939	0.942
6.20	0.965	0.961	0.984	0.981	0.949	0.952
6.65	0.970	0.967	0.983	0.983	0.958	0.956
7.10	0.977	0.974	0.986	0.985	0.964	0.966
7.60	0.982	0.981	0.989	0.988	0.970	0.973
8.00	0.989	0.988	0.996	0.995	0.979	0.982
8.50	0.984	0.979	0.989	0.986	0.979	0.968
8.90	0.866	0.844	0.924	0.914	0.919	0.916
9.30	0.792	0.777	0.881	0.890	0.904	0.899
9.75	0.768	0.753	0.890	0.889	0.898	0.901
10.1	0.716	0.696	0.887	0.868	0.979	0.873
10.5	0.687	0.668	0.867	0.869	0.856	0.852
10.9	0.717	0.702	0.886	0.865	0.832	0.836
11.3	0.718	0.705	0.882	0.860	0.814	0.834
11.7	0.748	0.737	0.876	0.900		0.821
12.1	0.732	0.716		0.876		0.832
12.5	0.783	0.773	0.898	0.886		0.859
13.0	0.831	0.809	0.886	0.906		0.868
13.5	0.830	0.826	0.924	0.927		0.924
14.0	0.817			0.926		
14.5	0.917			0.937		
15.0	0.863					

Table 10

Normal Spectral Emissivity of Silicon Nitride at 1800K

Wavelength (μm)	Sample/Trial: Airesearch First	Airesearch Second	Airesearch Third	Airesearch Fourth	Kyocera* First	Kyocera* Repeat
3.25	0.923	0.911	0.874	0.852	0.806	0.772
3.75	0.935	0.922	0.891	0.871	0.819	0.777
4.25	0.943	0.931	0.905	0.883	0.822	0.782
4.75	0.949	0.937	0.913	0.894	0.827	0.786
5.25	0.952	0.944	0.919	0.903	0.834	0.785
5.75	0.953	0.942	0.919	0.901	0.829	0.792
6.20	0.954	0.944	0.926	0.909	0.829	0.788
6.65	0.955	0.944	0.926	0.912	0.828	0.784
7.10		0.943	0.927	0.916	0.825	0.789
7.60		0.947	0.929	0.926	0.823	0.789
8.00		0.945	0.935	0.941	0.832	0.784
8.50		0.957	0.947	0.952	0.859	0.789
8.90		0.957	0.966		0.866	0.809
9.30		0.970	0.969		0.863	0.813
9.75		0.970	0.959		0.863	0.808
10.1		0.959	0.954		0.848	0.791
10.5		0.952	0.948		0.823	0.761
10.9		0.946	0.950		0.812	0.749
11.3		0.961	0.946		0.800	0.744
11.7		0.955	0.956		0.825	0.776
12.1		0.962	0.945		0.837	0.802
12.5		0.959	0.946		0.831	0.804
13.0		0.957	0.943		0.838	0.826
13.5		0.933	0.940		0.844	
14.0		0.960	0.932		0.820	
14.5			0.934		0.784	

*Virgin sample

Discussion of the Results

Silicon Carbide. It appears that the presence of boron/carbon causes a peak in the spectral emissivity data at about 10.5 μm followed by a valley at about 13 μm. This peak-valley may not be stable at 1900K and above in high vacuum, even though the material was sintered or hot-pressed at significantly higher temperatures but probably not under high-vacuum conditions. The presence of Al_2O_3 does not significantly affect the spectral character of the data. The emissivity of the β-phase material decreases markedly with increasing wavelength in contrast to α-SiC. Even in the β-phase material, it is conceivable that the presence of boron/carbon may be noted at about 11 μm by the presence of a plateau. However, further verification of this point is needed. In any event, it is obvious that spectral emissivity of silicon carbide can be controlled at the longer wavelengths for particular applications. Since the present samples were diamond ground, they exhibited a polished appearance. The recommended (provisional) values given by CINDAS [13] for average polished SiC at 1000 and 2400K are also shown in Fig. 21. These values are about 15% below the present values below 11 μm and include the peak-valley found in the present samples which contain boron/carbon.

Silicon Nitride. The spectral emissivity of all of the silicon nitride samples exhibited a maximum at 8 μm followed by a sharp decline to 11 μm and an increase from 11 to 14 μm. No relationships to impurities were noted, so it is concluded that this behavior is typical of Si_3N_4. The provisional curve by CINDAS [13] is included in Fig. 26 . The general features of the provisional curve agree with the present results, but this curve generally lies about 10% below the present results.

PUBLICATIONS

The following reports and publications have been prepared on the emissometer studies during sponsorship by AFOSR.

(1) PRL Report 116, "Spectral and Total Emissivity and Reflectivity at High Temperature," April 30, 1976, D. P. DeWitt, B. Hoenle, and R. E. Taylor.

(2) PRL Report 126, "Description of the PRL High Temperature Emissometer," November 1976, D. P. DeWitt, R. E. Taylor, and B. D. Hoenle.

(3) PRL Report 130, "Spectral and Total Emissivity and Reflectivity at High Temperatures," March 31, 1977, R. E. Taylor and D. P. DeWitt.

(4) PRL Report 136, "Spectral and Total Emissivity and Reflectivity at High Temperatures," Progress Report of AFOSR, September 15, 1977, D. P. DeWitt, R. K. Riddle, and R. E. Taylor.

(5) DeWitt, D. P., Taylor, R. E. and Riddle, T. K., "High Temperature Computer Controlled Emissometer for Spectral and Total Measurements on Conducting and Nonconducting Materials," ASME Proceedings Seventh Symposium on Thermophysical Properties, ASME, Washington, D.C., May 1977. (Available May 1978).

(6) DeWitt, D. P. and Taylor, R. E., "Spectral Emissivity of Silicon Carbide and Silicon Nitride at High Temperatures," High Temperature-High Pressures, under preparation.

CONTINUATION OF THE RESEARCH

The accomplishments of the research program during the past two years represent contributions to high temperature property measurement and materials technology. This experience and the measurement capability, will make possible the generation of new information useful in understanding material behavior.

In this section, we will briefly summarize the objectives for continuation of the research program as formally proposed in late 1977.

(1) Measurement Method Studies

We will treat some of the more fundamental aspects of the measurement method, like cavity quality determination. These studies help to establish greater confidence in the method and generate a basis for careful evaluation of the systematic errors.

(2) Measurements on New Ceramic Materials

Samples of silicon carbide and silicon nitride, made available to us upon request to several vendors, have been studied and results presented in this report. There are still some aspects of this study as previously discussed which need to be clarified. These materials represent state-of-the-art in high temperature ceramics and are under consideration for a number of uses in advanced high technology applications. Consequently a knowledge of their properties at high temperatures and their behavior under various environmental conditions is currently of great interest. We will continue to study these materials and attempt

to obtain samples of Boron Nitride and Silicon Nitride.

(3) Radiation Shielding for Higher Temperature Operation

The power available to heating a sample within the Multiproperty Apparatus is limited to 10 kW as a consequence of the cooling capacity of the vacuum enclosure and bus bar/vacuum-feed through current capacity. Using reasonable sample geometrics (for radiative property measurements) is is not possible to achieve routine generation at temperatures above 2500 K. In order to obtain levels of 2700 to 3000 K, it is necessary to reduce the radiated flux from the sample. It is not always possible to use shorter or smaller samples. Therefore, the most promising and practical appraoch is to use radiation shielding.

Previous experiences with shielding have pointed out a major pitfall, namely, that of seriously altering the temperature distribution in the sample. For example, with longitudinal cylindrical shields, coaxial with the sample along the upper and lower third of the sample length, the middle section of the sample (the test region) can be made to be nearly isothermal. However, the temperature of the sample in the region surrounded by the heat shields becomes extremely hot, causing sample failure - even though the test section is at a lower temperature.

In this phase of the proposed program, we will develop heat transfer models that will lead toward optimum radiation shield configurations. Particularly important will be the parametrics studies to predict longitudinal temperature distribution such that we will be able to extend operation to very high temperature levels. This study will involve analytical modeling and experimentation to provide test data.

(4) Method for Measuring Transparent Materials

The capability of the Multiproperty Apparatus to provide normal spectral emissivity measurements in nonmetallic samples was a major advancement in high temperature measurement technology. There are requirements of national importance to extend our capability to consider nonmetallics which are transparent or translucent. We will include as part of the proposed program, a feasibility study to consider ways in which the features of the Multiproperty Apparatus can be efficiently used to permit observations on such materials.

The first part of the study will involve a careful review of the literature with particular attention to apparatus design and requirements of sample size configuration. The major difficulties in studying the transparent materials are maintaining isothermal sample volumes and avoiding radiant flux originating from the sample heater from reaching the detector. Recent interest in transparent materials has sparked the development of a new method which minimizes both these effects by rapid removal of the sample from its furnace and high speed (ms) acquisition of the spectral radiance. This is a very complicated approach, well within the technology, but which would be too costly (to build and operate) to support materials development work. Consequently, we don't see a high-speed technique as the starting point for our feasibility study.

The direction of the study will be toward configuring a heating tube-sample arrangement that is compatible with existing electrodes on the Multiproperty Apparatus. It is likely that auxiliary heaters will be necessary to create the necessary enclosure for the sample and for

ancilliary blackbodies. One technique is suggested from our arrangement used to get emissivity of the nonconductors. The transparent material - in cylindrical-slug form - would be mounted within a heating tube and a lateral opening (hole) provided for the optical system to collect spectral radiance leaving the opening. The lateral opening size will have an effect on the temperature distribution in the sample; this effect will not be as great as predicted for an opaque nonconductor. We can look upon the sample-tube configuration in this manner: without a sample present, the lateral opening behaves as a high quality blackbody; the effect of the transparent sample is to modify this behavior. The first question is can we develop a model to relate the spectral radiance change to the spectral emissivity and geometry of the sample. This would be a good starting point for the feasibility study.

SUMMARY

The high temperature Multiproperty Apparatus at PRL is a powerful and unique tool for simultaneously measuring ten thermophysical properties on the same sample of an electrically-conducting solid and of studying its behavior under various environmental conditions. The addition of the ability to measure spectral emissivity from 0.3 to about 14 μm at temperatures up to 2700 K for both electrically conducting and insulating solids significantly enhances this Apparatus. This addition provides the capability for measuring the surface properties of materials of interest to laser weaponry. The Apparatus features rapid time-to-temperature and data acquisition under minicomputer control yielding state-of-the-art accuracy.

Spectral emissivity measurements to at least 10 μm have been made on tantalum (reference material), SiC, Si_3N_4, graphite and carbon-carbon composites from 1500 to 2400 K or their respective degradation temperatures. The new data on the ceramics provides some understanding on their high temperature behavior including the effect of fabrication process and impurities.

It is anticipated that emissivity research studies will continue and include extension of the temperature range to both higher and lower temperatures, extension to longer wavelengths (14 micrometers), and, most important, a feasibility study on measuring translucent materials.

REFERENCES

1. See "Thermophysical Properties of Aircraft Structural Materials in Solid and Molten States", Y. S. Touloukian and C. Y. Ho, Survey Report dated August, 1974.

2. Y. S. Touloukian and C. Y. Ho, editors, 1976, published by the Thermophysical and Electronic Properties Information Center, 2595 Yeager Rd., W. Lafayette, Indiana.

3. Powell, R. W. and Taylor, R. E., "Multi-Property Apparatus and Procedure for High Temperature Determination," Revue Internationale des Hautes Temperature et des Refractaires, 7, 298-304, 1970.

4. Riddle, T. K., "A New Method for Measuring the Spectral Emissivity of Nonconducting Materials at High Temperatures", M.S. Thesis, School of Mechanical Engineering, Purdue University, May 1978.

5 Larrabee, R. D., "Spectral Emissivity of Tungsten," J. Opt. Soc. Am. 49, 619-25, 1959.

6. Larrabee, R. D., "The Spectral Emissivity and Optical Properties of Tungsten," Research Laboratory of Electronics, Massachusetts Institute of Technology, TR 328, May 1957.

7. DeVos, J. C., "Evaluation of the Quality of a Blackbody," Physica 20, 669-89, 1954.

8. Taylor, R. E., Kimbrough, W. D., and Powell, R. W., "Thermophysical Properties of Tantalum, Tungsten, and Tantalum-10Wt. Percent Tungsten at High Temperatures", Journal of the Less Common Metals, 24, 369-382, 1971.

9. Riethof, T. R. and DeSantis, V. J., "Techniques of Measuring Normal Spectral Emissivity of Conductive Refractory Compounds at High Temperatures," Measurement of Thermal Radiation Properties of Solids (J. D. Richmond, Editor) NASA SP-31, p. 565-84, 1963.

10. Riethof, T. R., Acchione, B. D., and Branyan, E. R., "High-Temperature Spectral Emissivity Studies on Some Refractory Metals and Carbides," Temp. Meas. Control Sci. Ind. 3, Pt. 2, 515-22, 1962.

11. Riethof, General Electric Company, Space Science Laboratory, 1-34, 1961 [AD 250 274, TPRC No. 16963].

12. Kovalev, I. I., Muchnik, G. F., "Normal Spectral Emissivity of Tungsten, Niobium, Molybdenum and Tantalum in the Range of Wavelengths $\Delta\lambda$ from 0.66 to 5.12 microns and in the Temperature Range 1400-3000K," Teplofiz Vysok Temp., 8, 983, 1970.

13. Touloukian, Y. S. and Ho, C. Y., (Editors), "Thermophysical Properties of Selected Aerospace Materials, Part I: Thermal Radiative Properties" TEPIAC/CINDAS, Purdue University, 1976.

Appendix A

TABULATED RESULTS FOR TANTALUM MEASUREMENTS

Table A-1 Tantalum at 1930K, Fig. 14

$\lambda(\mu m)$	ε_λ
2	0.189
2.5	0.171
3	0.165
3.5	0.157
4	0.151
4.5	0.150
5	0.136
5.5	0.133
6	0.133
6.5	0.130
7	0.124
7.5	0.119
8	0.114
8.5	0.116
9	0.131
9.5	0.127
10	0.124
10.5	0.121
11	0.098
11.5	0.115

Table A-2 Comparison of Tantalum Data, Fig. 15

$\lambda(\mu m)$	Data Obtained 5/18/77 ε_λ	Data Obtained 1/21/78 ε_λ
2	0.205	0.230
2.5	0.182	0.201
3	0.175	0.188
3.5	0.167	0.179
4	0.162	0.170
4.5	0.155	0.166
5	0.149	0.167
5.5	0.145	0.154
6	0.145	0.146
6.5	0.138	0.141
7	0.132	0.136
7.5	0.133	0.127
8	0.141	0.122
8.5	0.123	0.121
9	0.121	0.116
9.5	0.115	0.113
10	0.141	0.112
10.5	0.127	0.098
11	0.117	0.101
11.5	0.108	0.088
12		0.084
12.5		0.087
13		0.078
14		0.063
14.5		0.061

Table A-3 Comparison of Tantalum Results with Existing Data, Fig. 16

	T = 1950K	T = 2275K
λ(μm)	ε_λ	ε_λ
2	0.1850	0.204
2.5	0.161	0.176
3	0.149	0.169
3.5	0.145	0.157
4	0.138	0.152
4.5	0.131	0.143
5	0.126	0.136
5.5	0.117	0.130
6	0.107	0.123
6.5	0.114	0.116
7	0.108	0.114
7.5	0.095	0.109
8	0.087	0.103
8.5	0.080	0.100
9	0.080	0.084
9.5	0.070	0.088
10		0.086
10.5		0.082

Appendix B

SUPPLIERS OF THE CERAMIC SAMPLES

Silicon Carbide

Ceradyne, Inc.
P.O. Box 11030
Santa Ana, CA 92705
Attn: Jack Rubin

The Carborundum Co.
P.O. Box 1054
Niagara Falls, NY 14302
Attn: Dr. Edwin Kraft

General Electric Co.
Research and Development Center
P.O. Box 8
Schenectady, NY 12301
Attn: C. A. Johnson
Physical Chemistry Laboratory
Ceramics Branch

Silicon Nitride

Airesearch Casting Co.
3525 West 190th Street
Torrance, CA 90509
Attn: M. Rorabaugh

Kawecki-Berylco Industries, Inc.
P.O. Box 1462
Reading, PA 19603
Attn: Robert J. Longenecker

Kyocera International, Inc.
8611 Balboa Avenue
San Diego, CA 92133
Attn: Bill Everett

SECURITY CLASSIFICATION OF THIS PAGE (When Data Entered)

REPORT DOCUMENTATION PAGE

READ INSTRUCTIONS BEFORE COMPLETING FORM

1. REPORT NUMBER: AFOSR-TR-78-0901	2. GOVT ACCESSION NO.
3. RECIPIENT'S CATALOG NUMBER	
4. TITLE (and Subtitle): SPECTRAL AND TOTAL EMISSIVITY AND REFLECTIVITY AT HIGH TEMPERATURES.	5. TYPE OF REPORT & PERIOD COVERED: INTERIM rept. (Annual), 1 Feb 77 - 31 Jan 78
6. PERFORMING ORG. REPORT NUMBER: PRL-152	
7. AUTHOR(s): D P DEWITT, T K RIDDLE, R E TAYLOR	8. CONTRACT OR GRANT NUMBER(s): AFOSR-77-3280 new
9. PERFORMING ORGANIZATION NAME AND ADDRESS: PURDUE UNIVERSITY, PROPERTIES RESEARCH LABORATORY WEST LAFAYETTE, IN 47906	10. PROGRAM ELEMENT, PROJECT, TASK AREA & WORK UNIT NUMBERS: 2308B1, 61102F, B1
11. CONTROLLING OFFICE NAME AND ADDRESS: AIR FORCE OFFICE OF SCIENTIFIC RESEARCH/NA, BLDG 410, BOLLING AIR FORCE BASE, D C 20332	12. REPORT DATE: 03 Apr 78; 13. NUMBER OF PAGES: 86 (87 p.)
14. MONITORING AGENCY NAME & ADDRESS (if different from Controlling Office)	15. SECURITY CLASS. (of this report): UNCLASSIFIED
	15a. DECLASSIFICATION/DOWNGRADING SCHEDULE

16. DISTRIBUTION STATEMENT (of this Report)

Approved for public release; distribution unlimited.

17. DISTRIBUTION STATEMENT (of the abstract entered in Block 20, if different from Report)

18. SUPPLEMENTARY NOTES

19. KEY WORDS (Continue on reverse side if necessary and identify by block number)

METALS
CERAMICS
THERMAL RADIATIVE PROPERTIES
SURFACE PROPERTIES
THERMOPHYSICAL PROPERTIES
EMISSIVITY
BRIGHTNESS

20. ABSTRACT (Continue on reverse side if necessary and identify by block number)

The status of the high temperature emissometer at the Properties Research Laboratory is described in detail. The emissometer is an extension of the multiproperty apparatus which is a powerful and unique tool for simultaneously measuring ten thermophysical properties on the same sample of an electrically-conducting solid and of studying its behavior under various environmental conditions. The apparatus features rapid time-to-temperature and data acquisition under minicomputer control yielding state-of-the-art accuracy. Performance evaluation tests of the emissometer are presented. These tests deal with veiling glare, black-body cavity quality, and temperature distribution in the heating tube.

* SEE ABSTRACT IN FRONT OF DOCUMENT

DD FORM 1 JAN 73 1473 EDITION OF 1 NOV 65 IS OBSOLETE

UNCLASSIFIED

SECURITY CLASSIFICATION OF THIS PAGE (When Data Entered)

408 947